Fetal cardiac output and its distribution to the placenta and brain at 11-20 weeks of gestation

Tommi Vimpeli MD

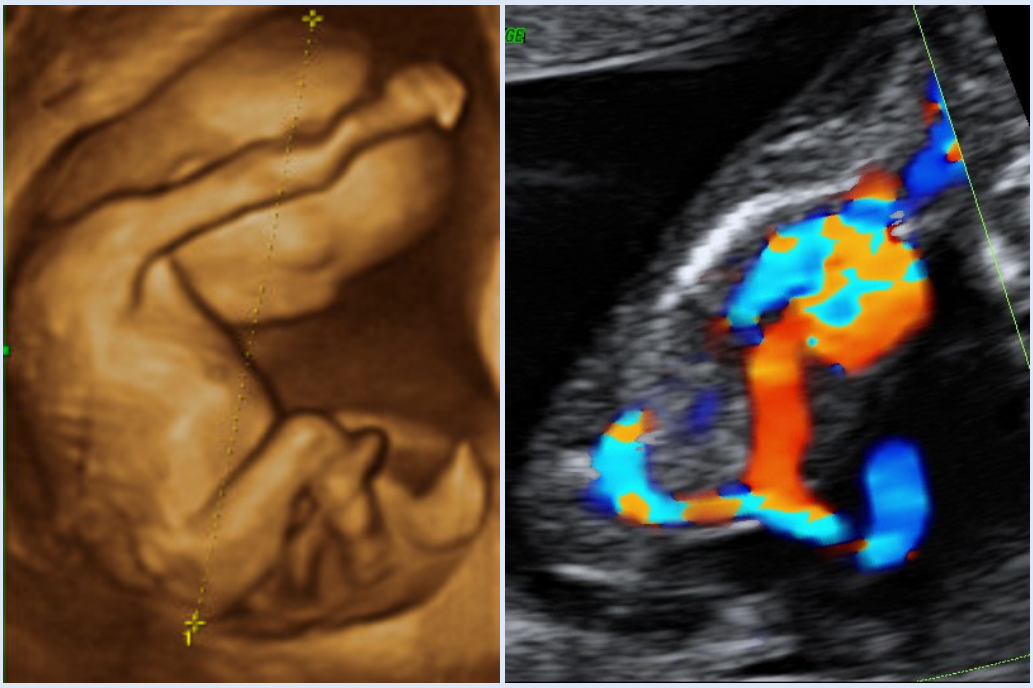

A dissertation for the degree of Philosophiae Doctor

UNIVERSITY OF TROMSØ
Faculty of Medicine
Institute of Clinical Medicine

September 2009

Fetal cardiac output and its distribution to the placenta and brain at 11-20 weeks of gestation

Tommi Vimpeli MD

A dissertation for the degree of Philosophiae Doctor

UNIVERSITY OF TROMSØ
Faculty of Medicine
Institute of Clinical Medicine

September 2009

+

CONTENTS

ACKNOWLEDGEMENTS

First and foremost I would like to thank my principal supervisor Professor Ganesh Acharya. After our first meeting we decided to do research, utilize the daily work I do. He was right convincing me that it will give me broader vision on the work and along with it my skills will improve. He is a supervisor who makes you work and this I mean in most positive way. Ganesh has been involved with this work from the start to finish, he has taught me to do ultrasound, to do research, to write and taught me to write well, he has sent me abroad, he has fed me at his home. I hope that he has found this work useful also, and we will continue to collaborate in the future

Hanna Portimojärvi, we came for a visit to Tromsø after we lived a period there. You took me to meet Professor Ganesh Acharya. You are partly responsible for this work ever taking place. Warm thank you and for your spouse Petri, too. He has also helped me in many ways. We have enjoyed Bergen “fiskesuppe” with appropriate barley drinks with Hanna and Petri and felt very welcome every time.

I wish to thank my former "boss" Aki Kuukankorpi for creating a workplace suitable to do this work and thus enabling the whole project. He supported my projects from the start, seeing that research can be done everywhere a patient meets a specialist. He has been most positive towards this work and pulled a rabbit out of a hat more than once in setting up the physical framework for me. He is a wizard in utilizing recourses and can squeeze water from a rock. He has also a remarkable quality of getting the best of skilled workers and making them feel important. He sees his leadership through the people working with him and through their skills. Special thanks go to his grandson for letting me take pictures of his heart for the Study I.

Heini Huhtala has been untiring in helping me with all possible questions with statistics, and she has always found time for me for the numerous visits regarding these studies. She has said that I have evolved in this area, I hope she is not just polite. Tom Wilsgaard analyzed all longitudinal data, he has done an enormous work with all variables and equations.

Professor Jan Martin Maltau has helped me as the co-supervisor. I am very grateful to him for making it possible for me to attend several courses and supporting the framework of this project.

I wish to thank my Swedish colleague Pediatric Cardiologist Sven-Erik Sonesson for welcoming me to Astrid Lindgren Hospital for Children, Stockholm, for a clinical attachment and providing invaluable guidance on fetal heart examinations.

Maternity Clinic at the University Hospital of Northern Norway has always taken extra good care of me, Jorunn Hansen, Annbjørg Tretten and Gun Jensen. They have helped me with all possible things starting from "where is Ganesh?" to where can you get "tørr torsk". I hope Turid S. Bakkevoll does not see ghosts after completing the final form of this thesis, she deserves a special thank for helping me with the "grand finale".

I wish to thank Kimmo Lahti, Heidi Liikkanen and Seppo Valli from GE Health Care for the technical support they provided during the period of this research. Jarmo Lieto from Sonar OY deserves a special thank for helping me with matters concerning ultrasound machines. I also wish to thank Tuomo Noukkala from Tosfin OY for reviewing the technical part of ultrasound and Doppler in this thesis.

Tampere university library and the personnel in the Department of Health Sciences have helped me many times finding material, sometimes several years old outside ancient internet age.

Rahku Marathon Club and Petomaanit are groups of people I am able to spend a part of my leisure time with. Life is not just work and research. The time I have spent with you except the last two kilometres before finish line in marathon have given me extra energy for other aspects of life, for this work too.

Riitta and Aimo Auvinen, my wife's parents, thank you for helping our family on the many occasions this work has taken me away from home, for all the help and support you have given us all the way. Our children have the finest grandparents one can wish for.

Butch and Nova Jean Miller, part of this project started at 7311 Paul Street and at Laker High. Thank you for "adopting" me as a member of your family.

I wish to present my mother Salme Vimpeli. She is a person who never makes "a number of her", but her devotion to her children is complete. She has told me if you do something why not do it well and make yourself useful at the workplace. On the other hand she says that a good book and a pause will be as useful. Life is a balance. She has supported me all the way in my career, as have my brothers Jouni, Sauli and Veli-Matti and our sister Kristiina. I also thank their spouses and children, we are a big bunch and that is something.

I have done this project on the side of full day clinical work and it has required quite a lot of effort and time away from other aspects of life, most importantly from our family. This would have not been possible without my wife Sanna-Mari. She is the element

behind my success. She has taken care of the family and her own work, and at the same time she advices me on research matters and she has done research herself. She is a wizard of utilizing the mere 24 hours of a day. Sanna-Mari has guided me all the way and given often comments not so nice, but well deserved. I would have not accomplished this work without her and I love her for that too. She is the Mother and makes our home Home for us and for our children Tuomo, Eeva and Kaisa.

सर्वप्रथम मेरो प्रमुख सुपरभाइजर (प्रवेक्षक) प्राध्यपक गणेश आचार्यज्युमा म धन्यवाद प्रकट गर्न चाहन्छु। हाम्रो पहिलो अनौपचारिक भेटघाटमा मेरो दैनिक कार्यको विषयमा अनुसन्धान गर्ने निर्णय हामीले गर्यौं । यहाँको निरन्तर हौसला र प्रेरणाले मलाई यो विषयमा अझै केही गर्ने उत्प्रेरणा जगाय्यो। यहाँजस्तो पर्यवेक्षकसँग काम गर्दा धेरै कुरा अनुभव गर्ने र येस्ले मेरो काममा धेरै नै सकारात्मक प्रभाव परेको छ। मलाइ विश्वास छ कि यहाँले पक्कै पनि यो कार्यलाई उपयोगी पाउनुहुन्छ अनी आगामी दिनहरुमा पनि यसरी नै साझेदारीमा काम गर्न पाउने कुरामा आशावादी छु।

Tromsø, September 2009

Tommi Vimpeli

ABBREVIATIONS

AI	aortic isthmus
CCO	combined cardiac output
CO	cardiac output
CSA	cross-sectional area
DV	ductus venosus
EDV	end-diastolic velocity
ET	ejection time
FHR	fetal heart rate
FT	filling time
ICT	isovolumic contraction time
IRT	isovolumic relaxation time
IVC	inferior vena cava
LPV	left portal vein
LVCO	left ventricular cardiac output
PI	pulsatility index
PSV	peak systolic velocity
Q	volume blood flow
RI	resistance index
RVCO	right ventricular cardiac output
TAMXV	time-averaged maximum velocity
TAV	time-averaged intensity weighted mean velocity
UA	umbilical artery
VTI	velocity time integral
UV	umbilical vein

ABSTRACT

Objective

To study some aspects of fetal heart structure and function using ultrasonography at 11-20 weeks of gestation with an emphasis on the distribution of cardiac output to the placenta and upper body including brain.

Methods

In a cross-sectional study of unselected pregnant population, the structure of the fetal heart was studied using transvaginal ultrasonography and feasibility of obtaining standard echocardiographic views and measuring different structures was evaluated in 584 fetuses at 11+0-13+6 weeks of gestation. Reference ranges were established for the heart/ thorax circumference ratio, ventricular size and the diameters of the aorta and main pulmonary artery at the respective semilunar valve levels.

The fetal cardiac function was studied in a prospective longitudinal study of 143 pregnant women from an unselected population who were serially examined three times during 11-20 weeks of gestation. Blood flow velocities and diameters of the main pulmonary artery, aorta, aortic isthmus and umbilical vein were measured using pulsed-wave Doppler and B-mode ultrasonography, respectively and the reference ranges were constructed. The volume blood flow (Q) was calculated as a product of mean velocity and cross-sectional area of the vessel. Reference intervals were established for the umbilical vein (Q_{uv}) and aortic isthmus (Q_{ai}) volume blood flows and the left (LVCO), right (RVCO) and combined (CCO) ventricular cardiac outputs. The fraction of CCO distributed to the placenta was calculated as: Q_{uv}/CCO*100 and the fraction of CCO distributed to the upper body and brain was calculated as: (LVCO – Q_{ai})/CCO*100.

Results

It was possible to study the fetal heart anatomy by obtaining standard echocardiograhic views using transvaginal ultrasonograpy in a majority of cases in the late first trimester. The cardiac ventricles and their outflow tracts showed a linear growth with advancing gestational age during 11-14 weeks of gestation.

The CCO increased 1.9-fold from 11 to 20 weeks of gestation and the placental volume blood flow almost tripled during the same period. The fraction of CCO diverted to the placenta increased from 14% at 11 weeks to 21% at 20 weeks.

Aortic isthmus had a positive forward flow during the whole cardiac cycle during 11-20 weeks of gestation. Aortic isthmus blood flow velocities as well as the diameter

increased with advancing gestation, resulting in a significant increase in Q_{ai} from 1.9 to 40.5 ml/min during 11-20 weeks. However, the fraction of CCO directed to the upper body including brain remained relatively stable (approximately 13%) during this gestational period.

Conclusion

It appears feasible to study fetal heart anatomy in late first trimester using transvaginal echocardiography and to confirm normality. We have established references ranges for the evaluation of some cardiac structures at 11-14 weeks of gestation and for the serial measurement of Q_{uv}, Q_{ai} and cardiac ventricular outputs at 11-20 weeks of gestation. Placental volume blood flow and the fraction of CCO distributed to the placenta increases substantially during 11-20 weeks of gestation reflecting faster placental growth relative to fetal growth and establishment of low resistance circulation during the first half of pregnancy. The fraction of cardiac output directed to the upper body and brain is relatively small but fairly constant during 11-20 weeks of gestation.

LIST OF ORIGINAL PAPERS

I. Vimpeli T, Huhtala H, Acharya G. Fetal echocardiography during routine first-trimester screening: A feasibility study in an unselected population. *Prenat Diagn. 2006;26:475-82.*

II. Vimpeli T, Huhtala H, Wilsgaard T, Acharya G. Fetal cardiac output and its distribution to the placenta at 11-20 weeks of gestation. *Ultrasound Obstet Gynecol. 2009;33:265-71.*

III. Vimpeli T, Huhtala H, Wilsgaard T, Acharya G. Fetal aortic isthmus blood flow and the fraction of cardiac output distributed to the upper body and brain at 11-20 weeks of gestation. *Ultrasound Obstet Gynecol. 2009;33:538-44.*

INTRODUCTION

The fetal circulation is characterized by the presence of low resistance placental and high resistance pulmonary circulations. During intrauterine life, the gas exchange takes place in the placenta rather than in the lungs. A significant volume of blood is contained extra-corporally (within the placenta). Additionally, the fetal circulation differs from the postnatal circulation due to the unique intrinsic characteristics of fetal myocardium, parallel arrangement of the ventricular pumps, and the presence of physiological "shunts" and "watershed" areas that allow appropriate mixing and adequate distribution of blood to the organs and tissues. Advances in ultrasound imaging technology have made it possible to study fetal circulation non-invasively *in vivo* under physiological conditions. This has allowed us to update the existing concepts derived from data obtained invasively from experimental animal models and previable human fetuses. While new observations have confirmed the previous findings in many cases, in some instances they have given a completely different insight into the human fetal circulatory physiology. The studies presented in this thesis were performed to investigate certain aspects of fetal cardiovascular physiology in human fetuses during the first half of pregnancy.

NORMAL INTRAUTERINE DEVELOPMENT

Heart

Heart is formed in a fashion where components are added in a sequence to an initial primary structure, the cardiac crescent (Figure 1). The first step in the heart development is the formation of two heart fields of precardiac mesoderm, which are situated on opposite sides of the primitive foregut situated at the embryonic midline and contain endocardial as well as myocardial precursor cells. The first or the posterior heart field contributes to the bulk of the left ventricle and the secondary or the anterior heart field forms the right ventricle, outflow tracts, sinus venosus and atrial chambers (Bruneau, 2008). As the embryo develops, the heart fields fuse to form the primary heart tube, which connects at the cephalic end with the developing aortic arch system, and caudally with the vitelline and umbilical venous systems (Reller et al, 1991). The developing embryonic heart starts to contract about 20 days after conception (Bruneau, 2008) although the circulation is not yet established. Soon after the initiation of heart beat, the cardiac tube undergoes a process of looping and chamber formation (Sedmera & McQuinn, 2008). Gradual disappearance of cardiac jelly from the future cardiac chambers and accumulation in the atrioventricular junction and in the

developing outflow tract area leads to the formation of endocardial cushions (Wessels & Sedmera, 2003).

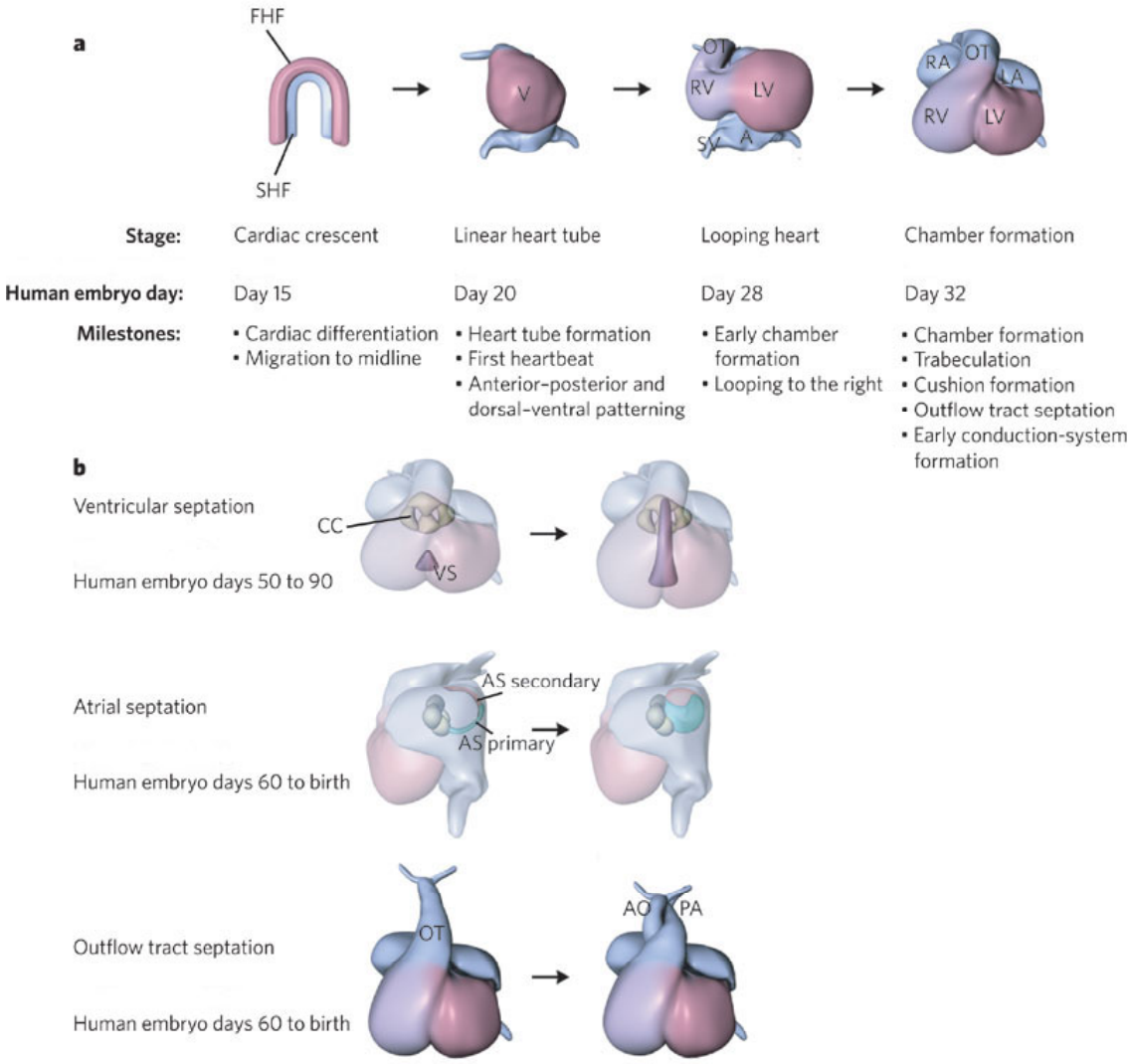

Figure 1. Steps in the development of human heart in chronological order (embryo days represent number of days after conception): a) early development b) maturation. FHF = first heart field, SHF = secondary heart field, V = ventricle, OT = outflow tract, RV = right ventricle, LV = left ventricle, SV = sinus venosus, A = atrium, RA = right atrium, LA = left atrium, CC = cardiac cushions, VS = ventricular septum, AS = atrial septum, PA = pulmonary artery, AO = aorta. Figure modified and reproduced with permission from Benoit G Bruneau. *Nature* 2008;451:943-8.

Further the atrioventricular valves develop from the cardiac cushions, and the interventricular septum arises from the left and right ventricular myocardium. Atrial septation occurs by the growth of primary and secondary septa. The common outflow tract is separated into the right (pulmonary artery) and left (aorta) by septation. The pulmonary veins and the

vena cavae connect to the left and right atria, respectively. There are further additions from the cardiac neural crest that contribute to the aortic arches and coronary vasculature (Cook et al, 2004, Moorman et al, 2003). The development of major structures of the heart is complete by eight weeks of gestation but the maturation and growth continues throughout the pregnancy.

Fetal heart is 8 mm long and positioned normally within the chest by 12 weeks, and by mid-gestation it is 24 mm in length (Cook, 2001). The size and weight of the heart relative to body size is higher in the fetus than in the adult.

Brain

Development of the fetal central nervous system starts two weeks after conception and continues beyond birth. The primordium of the central nervous system, the neural tube, develops from the ectodermal neural plate. Appearance of the neural plate 2-3 weeks after conception (Carnegie stage 8) is the first sign of neurulation. Neural folding starts at stage 9 (3.5 weeks) and the folds fuse during stage 10 (4 weeks after conception) at the level of third to fourth somite, which corresponds to the future rhombocephalon. The openings between rostral and caudal neural folds are called the anterior and posterior neuropores, respectively. The rostral part of the neural tube develops into the brain and the rest of it develops into the spinal cord. Neural crest cells become the peripheral nervous system.

The three major divisions of the brain i.e. the prosencephalon (forebrain), mesencepalon (midbrain) and rhombencephalon (hindbrain) appear in the walls of completely open neural groove three and half weeks after conception (Stage 9) (O´Rahilly & Muller, 2008). The anterior neuropore closure is completed during stage 11 (Yoon et al, 1997). The closure of the posterior neuropore takes place at the end of 4^{th} postconceptional week (stage 12). The final site of neural closure is at the future mid-lumber level.

The process of encephalization occurs during the 5^{th} postconceptional week (stage 13-15). The prosencephalon is divided into telencephalon (develops into the cerebral cortex, basal ganglia, amygdala, hippocampus and lateral ventricles) and diencephalon (develops into thalamus, hypothalamus, foramen of Monro and third ventricle). The mesencephalon forms tectum, tegmentum and cerebral aqueduct. Rhombencephalon divides into metencephalon (cerebellum, pons and fourth ventricle) and myelencephalon (medulla oblongata and fourth ventricle).

The process of elongation of caudal neural tube through the formation of a lumen (canalization) occurs during stages 13-20 (5-9 weeks after fertilization), when the notochord and the caudal end of neural tube merge.

Choroid plexuses differentiate during 8th postconceptional week (stage 18) (Muller & O´Rahilly, 2006) in the lateral ventricles and the roofs of the third and fourth ventricles and produce cerebro-spinal fluid. Foramina of Magendie and Luschka are formed around mid-gestation allowing the cerebro-spinal fluid to flow into the subarachnoid space.

The growth of the brain is slower in the second and third trimester compared to first trimester. However, there is nearly a 40-fold increase in weight of the brain between the end of the embryonic period and birth (O´Rahilly & Muller, 2008). The fetal brain appears to grow in a relatively constant manner throughout the gestation. Brain constitutes about 15% of the body weight in the first half of pregnancy among fetuses weighing between 1g and 500g (Tanimura et al, 1971) and about 13% of body weight in the second half of pregnancy (Walsh et al, 1974) compared to ~2% of body weight in adult humans (Dekaban 1978).

Placenta

Placenta and umbilical cord develop from trophoblasts and mesodermal chorion and allantois. Trophoblasts invade basal decidua and spiral arteries with subsequent destruction of the muscle and elastic elements. Trophoblast cells form the border between the mother and the fetus. Trophoblast cells grow together to form multinucleated syncytiotrophoblast cells and further placental villi. In the villi fetal blood vessels grow from the allantois. Placental villi arise secondary as a protrusion of cytotrophoblast into an already established syncytial network. Villus formation is completed by the 17th postconception day (Molteni et al, 1978). During the first half of pregnancy placenta undergoes some characteristic structural changes leading to a significant reduction in the size (from 140µ to 70µ) and increase in the number of chorionic villi. At term the chorionic villus has a size of approximately 50µ and the total villi surface area is about 13-14 m^2, which is ten times greater than the human skin surface area (Walsh et al, 1974)

The basic configuration of the placenta is formed by the end of the first trimester (Sariola et al, 2003), but it continues to grow until term. However, placental growth is slower than the fetal growth in the third trimester of pregnancy, where as the opposite is true for the first and second trimester. The ratio of placental weight to fetal weight decreases from 0.20 in the late second trimester to 0.15 at term (Walsh et al, 1974). Placenta grows linearly in

thickness during 8 to 20 weeks, from a mean thickness of 5.4 mm to 21 mm (Tongsong & Boonyanurak, 2004). The mean placental weight increases from 42g at 11 weeks to 157g at 20 weeks and the umbilical cord length increases from 11 cm to 30 cm during the same gestational period (Gilbert-Barness & Debich-Spicer, 2004).

SONOGRAPHIC ANATOMY

Fetal heart

Visceral situs and position of the heart

Situs is the location that an organ occupies in a bilateral system of symmetry. In situs solitus, inferior vena cava lies to the right and anterior to the spine and aorta is to the left. The stomach is on the left side of the upper abdomen and the liver and portal veins are on the right side (Figure 2).

Fetal heart is positioned in the chest more to the left side (levocardia). Between gestational age 8-11weeks fetal heart is actually positioned so that the right chamber is towards the right, left chamber to the left and apex pointing towards the sternum (Cook, 2001). By the end of week 12, heart has rotated so that the right chamber is towards the sternum and the apex of the heart points approximately 45 degrees to the sagittal and coronal planes. At mid-gestation fetal heart is almost transversally positioned, due to large fetal liver which extends from left to right in the upper part of the abdominal cavity (Cook et al, 2004).

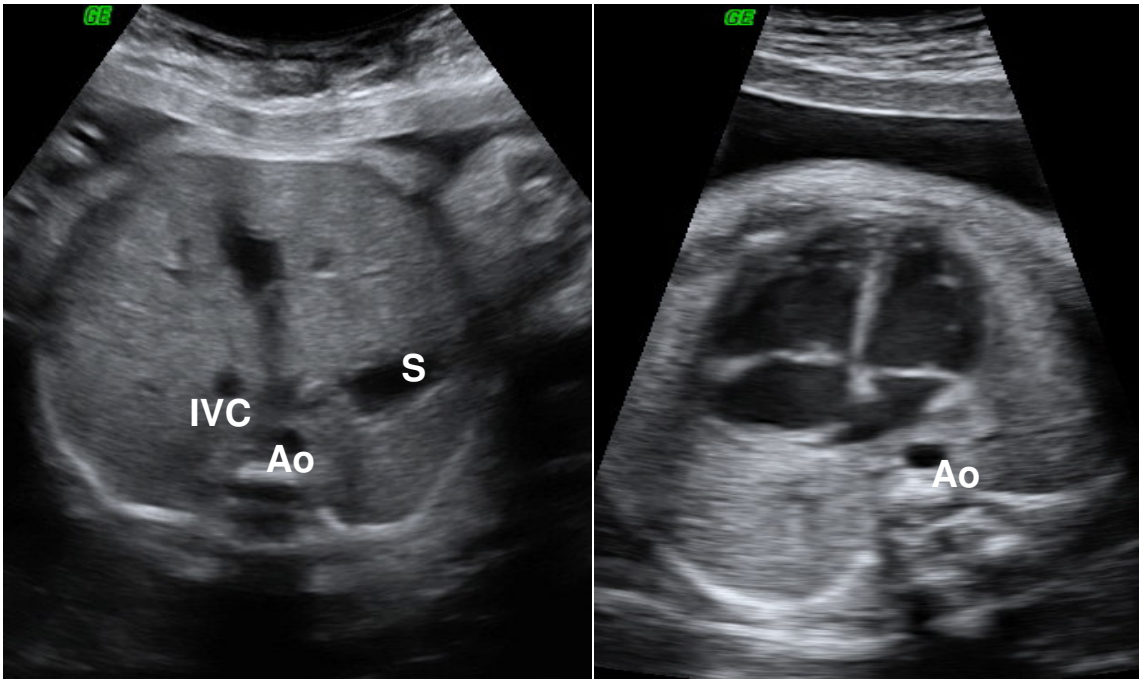

Figure 2. Transverse section of the abdomen (left) and chest (right) of a fetus in breech presentation demonstrating situs solitus and levocardia. Ao = Aorta, IVC = inferior vena cava, S = stomach.

Atria

It is important to establish the atrial situs and arrangement (the position of each atrium in relation to each other) during fetal echocardiography (Carvalho et al, 2005). Morphologically right atrium has a broad based triangular appendage. Left atrial appendage is tubular, hooked and has a narrow base. However, these characteristics may be difficult to demonstrate during fetal echocardiography, especially in early pregnancy. In usual atrial arrangement, inferior and superior vena cava drain to the right atrium and pulmonary veins drain to the left atrium. The coronary sinus is usually visible in the left atrioventricular groove and drains to the right atrium.

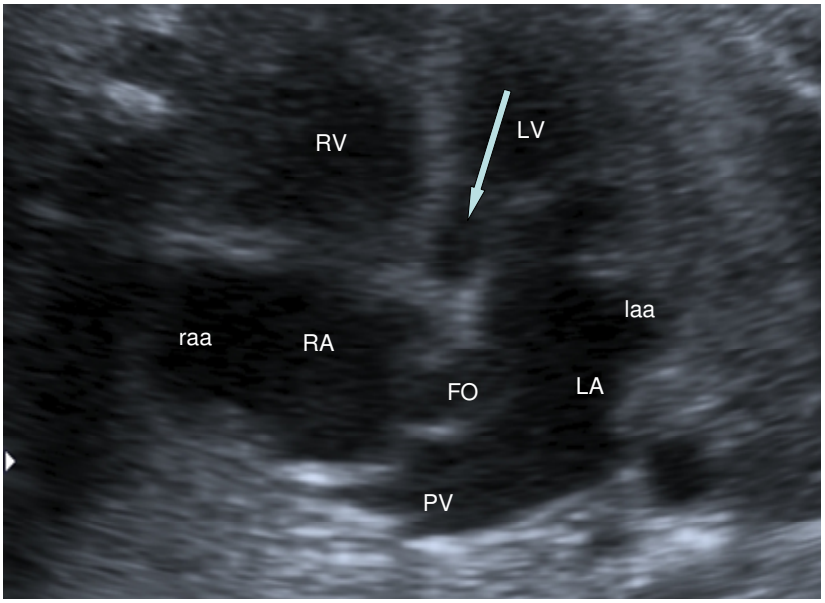

Figure 3. Ultrasound image of a fetal heart demonstrating two atria and their typical structures. RA=right atrium, raa= right atrial appendage (has a broad-based and is triangular), LA=left atrium, laa=left atrial appendage (has a narrow base and is tubular and hooked), pulmonary vein=PV drain into left atrium. FO = foramen ovale, RV=right ventricle, LV=left ventricle, arrow shows the left ventricular outflow tract.

Ventricles

The ventricles are normally equal-sized and are separated by an intact interventricular septum. The atria are connected to the ventricles via the atrioventricular valves. An atrioventricular connection exists when the cavity of an atrial chamber is in continuity with a ventricular cavity. In a concordant atrioventricular connection right atrium connects to the morphologically right ventricle and left atrium connects to the morphologically left ventricle.

Morphologically the right ventricle has coarser apical trabeculations than the left ventricle and a typical muscular bar (moderator band) is commonly present in the right ventricle. The left ventricle has smoother trabeculations and two papillary muscles that give a different appearance compared to the right ventricle.

In the right ventricle, septal leaflet of the tricuspid valve, attaches the cordae and papillary muscles to the interventricular septum. On the right side the atrioventricular valve is slightly more apical than on the left side.

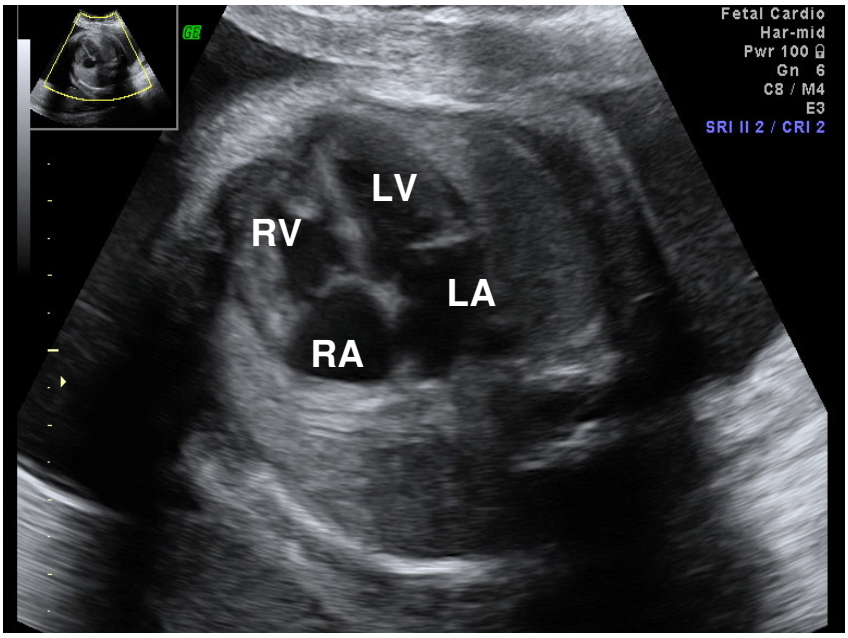

Figure 4. Four chamber view of a fetal heart demonstrating two equal sized atria and ventricles, (right ventricle is positioned anteriorly and has the moderator band), intact ventricular septum, two atrioventicular valves (the septal leaflet of the tricuspid valve is inserted more apically than that of the mital valve), crux of the heart with atrial septum, and foramen ovale.

Great arteries

The two great arteries are the aorta and the pulmonary artery. In concordant ventriculoarterial connection aorta is connected to the morphologically left ventricle and pulmonary artery is connected to the morphologically right ventricle. Two coronary arteries arise from the ascending aorta and the aortic arch gives three branches (brachiocephalic, left carotid and left subclavian arteries) that supply the head, neck and upper extremities.

Pulmonary artery bifurcates into left and right pulmonary arteries and continues as the arterial duct to connect the descending aorta. Aortic isthmus is located between the origin of the left subclavian artery and the connection of the arterial duct to the aorta.

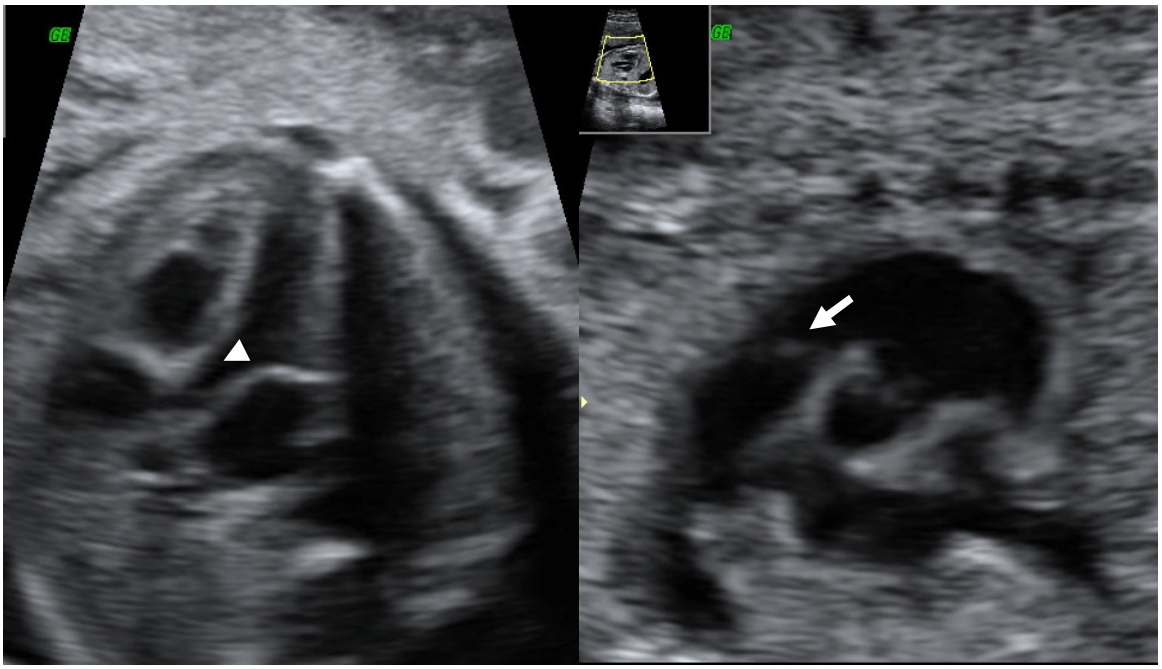

Figure 5. B-mode images of the cross-section of the fetal chest demonstrating the left (arrow-head) and right (arrow) ventricular outflow tracts.

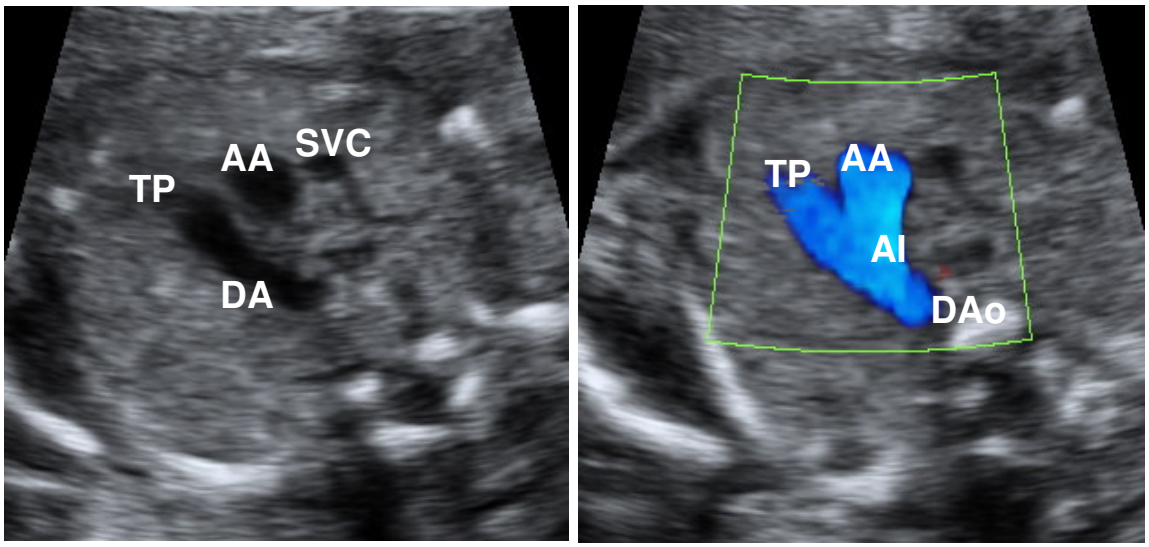

Figure 6. B-mode (left) and colour Doppler (right) images showing cross-sectional views of the fetal chest at the level of great arteries demonstrating the truncus pulmonalis (TP) and its continuation as the ductus arteriosus (DA) to join the descending aorta (Dao), the transverse aortic arch (AA) with aortic isthmus (AI) and the superior vena cava (SVC) in a so-called three-vessel view.

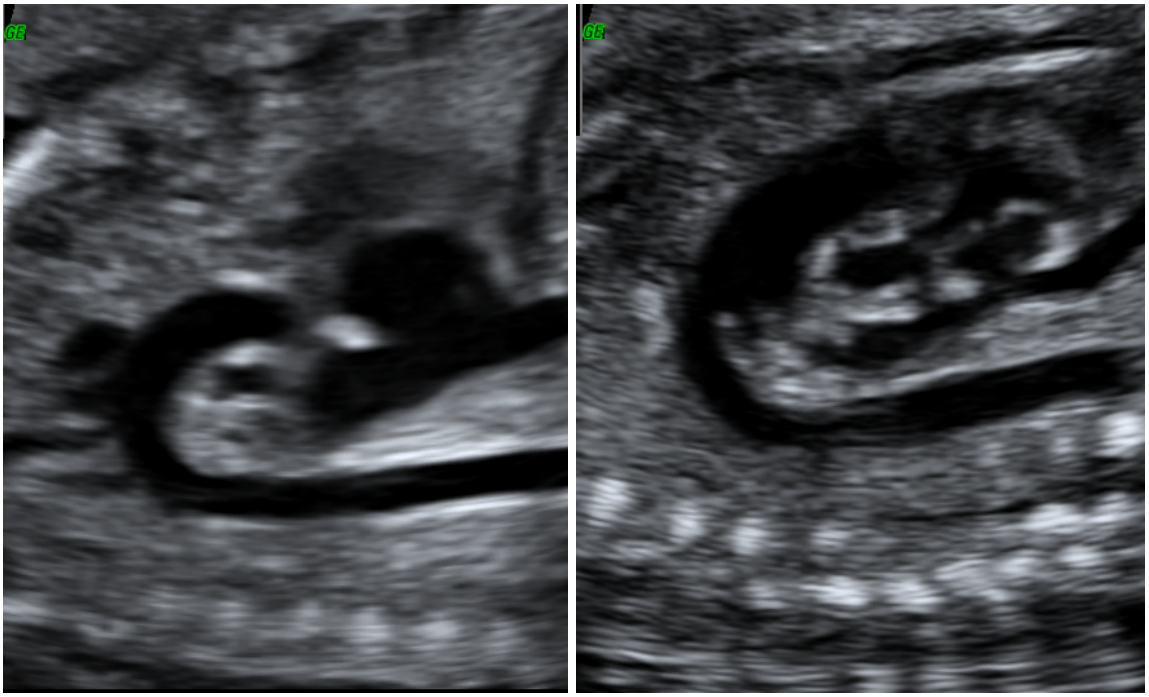

Figure 7. B-mode ultrasound image of the aortic arch with a typically hooked "candy cane" appearance demonstrating the origin of head and neck vessels (left) and pulmonary-ductal arch with a appearance typical "hockey stick" appearance (right). Reproduced with permission from G. Acharya. *Ultrasound Obstet Gynecol*. 2009 28;33:628-33.

Venous connections

Superior and inferior vena cavae connect to the right atrium and four pulmonary veins connect to the left atrium.

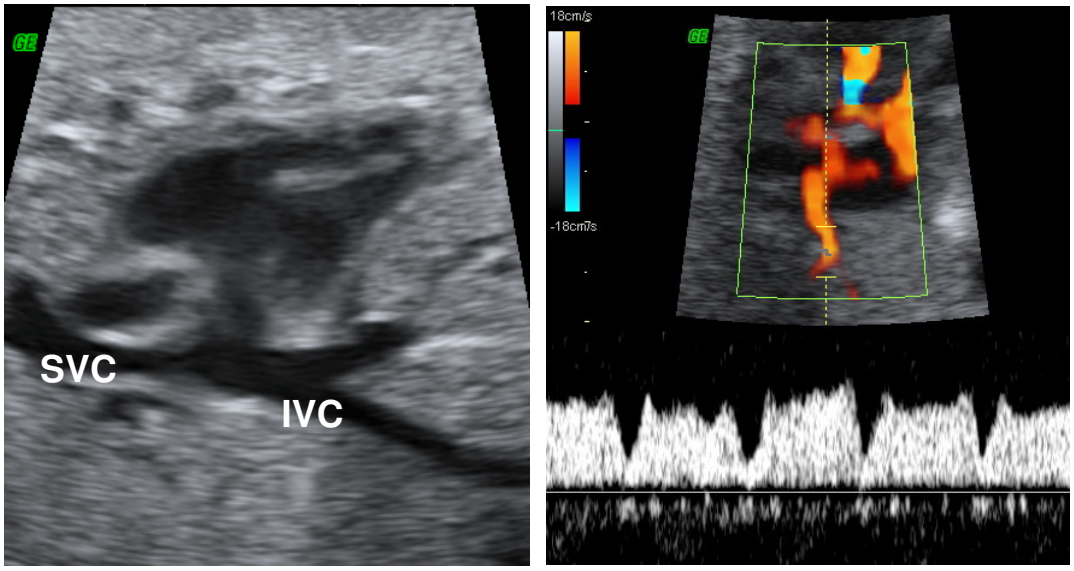

Figure 8. Longitudinal view of the fetal chest and upper abdomen demonstrating the connection of superior and inferior vena cavae to the right atrium (left) and colour Doppler image of the fetal heart demonstrating one of the pulmonary veins (Doppler sample volume is positioned at its proximal part) draining into the left atrium (right). Typical pulsed-wave Doppler velocity waveforms are shown in the lower panel.

Fetal brain

The ultrasonographic appearance of the embryonic/fetal brain in the first and second trimesters has been extensively reviewed recently by Blaas & Eik-Nes (2009) and Monteagudo & Timor-Tritsch (2009), respectively. Brain cavities can be identified as hypoechogenic structures as early as 7 weeks of gestation. Embryonic movements can also be detected at this stage (O´Rahilly & Muller, 2007). At 8 weeks, choroid plexus can be identified within the lateral ventricles, and a wide third ventricle and mesencephalic cavity are readily identifiable using transvaginal approach. At 9 weeks, the lateral ventricles are larger, choroid plexuses are brightly echogenic and easily recognized also in the fourth ventricle, diencephalic cavity becomes narrow and the falx cerebri can be imaged. A gap is seen between the rhombencephalic cavity and Sylvian aqueduct due to the growing cerebellum (Tanaka et al, 2000; Blaas & Eik-Nes, 2009).

During 10-13 weeks the cerebellum enlarges and becomes readily identifiable at 12 weeks with the two hemispheres joined at the midline. The lateral ventricles are filled with choroid plexus, and the cerebral hemispheres fill the anterior part of the head and conceal the diencephalic cavity. The third ventricle becomes increasingly narrow (Blaas & Eik-Nes, 2009). The corpus callosum is still not visible at this stage.

The landmarks that are identified and commonly assessed during ultrasonography of the fetal brain are shown in Figure 9. The cavum septi pallucidi, falx cerebri, anterior and posterior horns of the lateral ventricles with choroid plexuses, thalami, cerebellum, and cisterna magna are easily seen in the horizontal axial plane. The coronal and sagittal planes are better than the axial plane for studying median brain structures, such as interhemispheric fissure, corpus callosum, cavum septi pallucidi and frontal horns of the lateral venticles, choroid plexuses, third venticle, cerebellum and cerebral vermis.

The diameter of the anterior and posterior horns of the lateral ventricles is relatively constant (~ 7 mm) in the second and third trimesters (Pilu et al, 1989), whereas that of the cavum septi pallucidi decreases slightly with advancing gestation (Jou et al, 1998). The transverse cereberal diameter in mm corresponds approximately to the weeks of gestation in the second trimester (Hill, 1990). The third ventricle is easy to visualize between the thalami in the second trimester, but narrows progressively further during pregnancy. The fourth ventricle is usually covered by the cerebeller vermis by 18 weeks and may not be visible during ultrasonography. The cisterna magna measures about 5±3mm in the second and third trimester (Mahony et al, 1984).

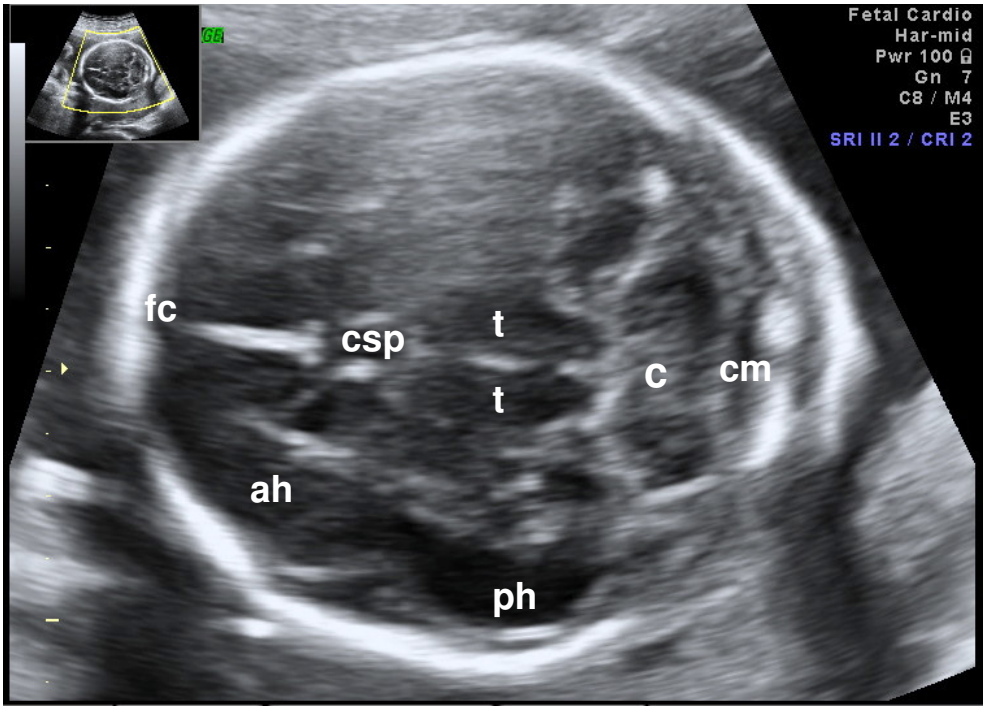

Figure 9. Cross-sectional image of the fetal head demonstrating falx cerebri (fc), cavum septi pallucidi (csp), thalamus (t), cerebellum (c), cisterna magna (cm) and the anterior (ah) posterior (ph) horns of the lateral ventricles. *Figure by the courtesy of G. Acharya.*

Placenta and umbilical cord

The human placenta has discoid shape and hemochorial interface. The weight of a term placenta is 500 – 600 g (normally 15-20% of the fetal body weight). It is 20 - 25 cm in diameter, 3 - 4 cm in thickness, 420 – 490 cm^3 in volume (Jackson et al, 1992) and has 15-25 distinct cotyledons on the maternal surface (Molteni, 1984). The placental growth is difficult to measure in vivo. However, placental volume has been measured with three-dimensional ultrasound. The placental volume correlates well with the gestational age and estimated fetal weight. In a recent study, the placental volume was shown to increase from 83 cm^3 at 12 weeks to 181.5 cm^3 at 20 weeks and 427.7 cm^3 at 40 weeks (de Paula et al, 2008).

Chorion frondosum that develops into definitive placenta can be identified as a thick echogenic structure as early as 6 weeks of gestation and is routinely identified for performing chorionic villus biopsy after 10 weeks of gestation in clinical practice. After 12 weeks, three distinct structures, i.e. chorionic plate, substance of the placenta and the basal layer, can be identified with B-mode ultrasonography. Changes in these structures are evaluated to study placental maturity using ultrasonography (Grannum et al. 1979).

The umbilical cord has two arteries and a single vein. Arteries are normally coiled around the vein (Figure 10). The length of the umbilical cord increases with gestation, from about 11 cm at 11 weeks to 30 cm at 20 weeks (Gilbert-Barness & Debich-Spicer, 2004) and reaches an average length of 55 - 60 cm at term (Naeye, 1985).

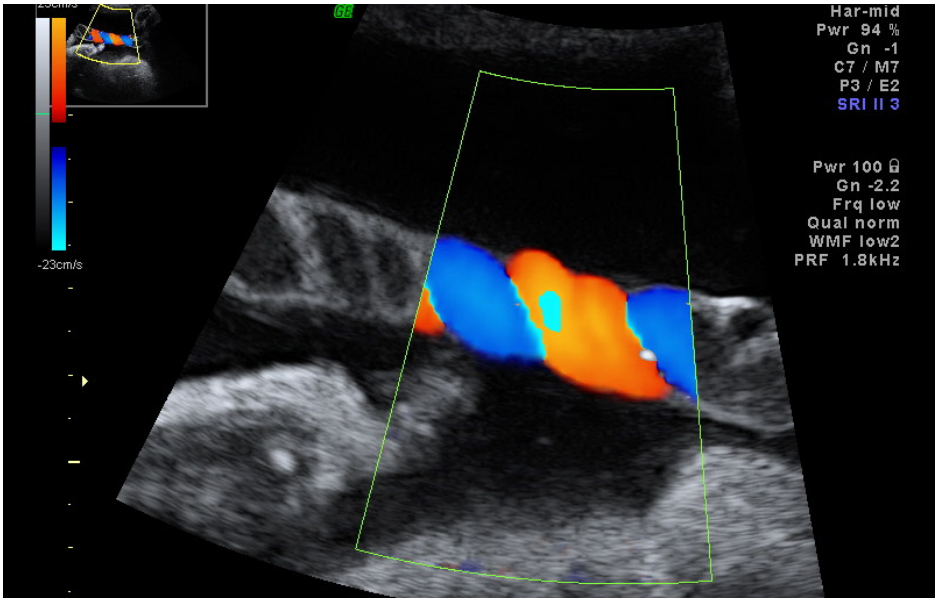

Figure 10. Colour Doppler image of a loop of the umbilical cord freely floating in the amniotic fluid demonstrating two arteries (red) typically coiled around a vein (blue). *Figure by the courtesy of G. Acharya.*

FETAL CARDIOVASCULAR PHYSIOLOGY

Cardiac function

Heart's main function is to deliver oxygenated blood and substrates to the tissues (Braunwald, 1977). The performance of the heart as a pump depends on intrinsic and extrinsic factors. The most important intrinsic factor is the contractile state of the myocardium. Extrinsic factors are heart rate, preload, afterload, ventricular interaction, extracardiac constraints and neurohumoral influences (Acharya et al, 2006).

Contractility is the ability of the myocardium to generate certain amount of pressure at a fixed amount of volume. At the cellular level contractility means Ca^{2+} mediated depolarization of the cardiomyocyte. The maximum force developed by a myocyte for a given length is representative of its contractility and the maximum pressure reflects the contractile performance of a ventricle at a given volume (Bers, 2002). Compared to adult, fetal myocardium contains fewer sarcomeres per myocyte (Friedman, 1972), the calcium uptake in the sarcoplasmic reticulum is less efficient (Mahony & Jones, 1986) and the maximal force that can be generated by the fetal myocardium is lower. First derivative of the maximal rate of ventricular pressure rise during the isovolumic period (dP/dt_{max}) is a commonly used index of contractility that can be assessed noninvasively in fetuses with atrioventricular valve

regurgitation using Doppler ultrasonography (Tulzer et al, 1991b, Huhta, 2004; Huhta, 2005). Normal dP/dt_{max} in human fetuses is approximately 1000 – 2000 mmHg/s.

Heart rate influences cardiac output linearly if stroke volume is held constant. An increase in heart rate can increase contractility and cardiac output, however the ventricular output decreases at heart rates >300-320/min. as the filling time decreases (Schmidt et al, 1995, Anderson et al, 1986, Anderson et al, 1987). In normal pregnancy, the fetal heart rate decreases from 175-180 beats/min at 9-10 weeks to 145-150 beats/min at 15 weeks of gestation (Ursem et al, 1998). The baseline heart rate varies normally between 110 and 150 beats/min during the last trimester of pregnancy. Fetal heart rate can vary significantly during fetal movements (Visser et al, 1982, Divon et al, 1985, Ball & Parer, 1992).

Preload is the amount of passive tension or stretch exerted on the ventricular walls just prior to the initiation of systole. In other words, it is the initial stretching of the myocardial fibres before contraction. Preload determines end-diastolic sarcomere length and therefore, the force of contraction. Commonly used surrogate measures of preload are ventricular end-diastolic pressure and atrial pressure. Preload of the left ventricle is determined mainly by the flow through foramen ovale and to lesser degree to pulmonary venous return. Preload of the right ventricle is determined by the flow of the inferior and superior vena cava (Acharya et al, 2006). Venous Doppler derived preload indexes (Kanzaki & Chiba, 1990) have been purposed but are not appropriately validated.

Afterload is the load the muscle faces during active force development, and it determines the degree of shortening. In functioning heart it refers to the systolic load on the ventricles. It is influenced by the peripheral vascular resistance, arterial pressure and arterial compliance. Afterload is the main determinant of myocardial oxygen consumption (Braunwald, 1971). In the fetal circulation, the afterload of the left ventricle is mainly determined by the resistance in the brachiocephalic circulation and that of the right ventricle in determined mainly by the resistance in the placenta and subdiaphragmatic circulation (Fouron, 2003; Acharya et al, 2006).

Although pressure measurements are used as surrogate indices of load, they may not be reliable as indicators of volume because ventricular compliance determines the volume at any particular pressure and the fetal myocardium is known to be less compliant than the adult (Rudolph, 2009). Additionally, the constraining effect of the pericardium, solid lungs and chest wall has a limiting effect on the stroke volume (Grant, 1999). Heart/chest circumference or area ratio measured using B-mode ultrasonography and ventricular shortening fractions measured by M-mode echocardiography can be used as noninvasive

surrogate measures of afterload in the fetus. Increased afterload may lead to cardiomegaly and cause an increase in heart/chest circumference ratio, which is normally 0.50 (Huhta, 2005). The mean heart/chest area ratio is shown to be 0.30 during the first half of pregnancy (Respondek et al, 1992). The shortening fractions of both ventricles remain constant (34±3%) throughout the second half of pregnancy (DeVore et al, 1984; Silverman & Schmidt, 1990). A reduction in right ventricular fractional shortening is seen in fetuses with increased afterload due to ductal constriction (Tulzer et al, 1991a) or placental insufficiency (increased placental vascular resistance) (Räsänen et al, 1989). Severely increased afterload may also cause tricuspid insufficiency, although prevalence of tricuspid regurgitation in normal fetuses is 4 - 7% (Respondek et al, 1994; Falcon et al, 2006).

Ratio between the ventricular inflow blood flow velocity during early filling and during the atrial contraction phase of the diastole (E/A ratio) have been used to assess the ventricular compliance (Tulzer et al, 1994). The E/A ratio increases with advancing gestation (Tulzer et al, 1994; Veille et al, 1999) mainly due to increase in E-wave velocity (Carceller-Blanchard & Fouron, 1993). The E/A ratio is approximately 0.5 at 13 weeks to 0.8 -0.9 at term (Wladimiroff et al, 1992; van der Mooren et al, 1991).

Other noninvasively measured parameters of cardiac function include volumetric flows (ventricular outputs), ventricular ejection force (Sutton et al, 1991; Rizzo et al, 1995), time intervals of the different phases of cardiac cycle and related indices, such as Tei index (Acharya et al, 2006). Ejection forces of both ventricles are equal and increase with gestation (Sutton et al, 1991; Rizzo et al, 1995; Räsänen et al, 1997). There is a significant increase in cardiac cycle length during 10 – 20 weeks of gestation. However, isovolumic contraction and relaxation times show a significant decrease (van Splunder & Wladimiroff, 1996). The proportion of the isovolumic time of the cardiac cycle is relatively constant in the second and third trimester (Tulzer et al, 1994) and the mean Tei index varies between 0.3 - 0.4 (Huggon et al, 2004; Hernandez-Andrade et al, 2007). The right ventricular ejection time is longer and the filling time shorter compared with the left ventricle.

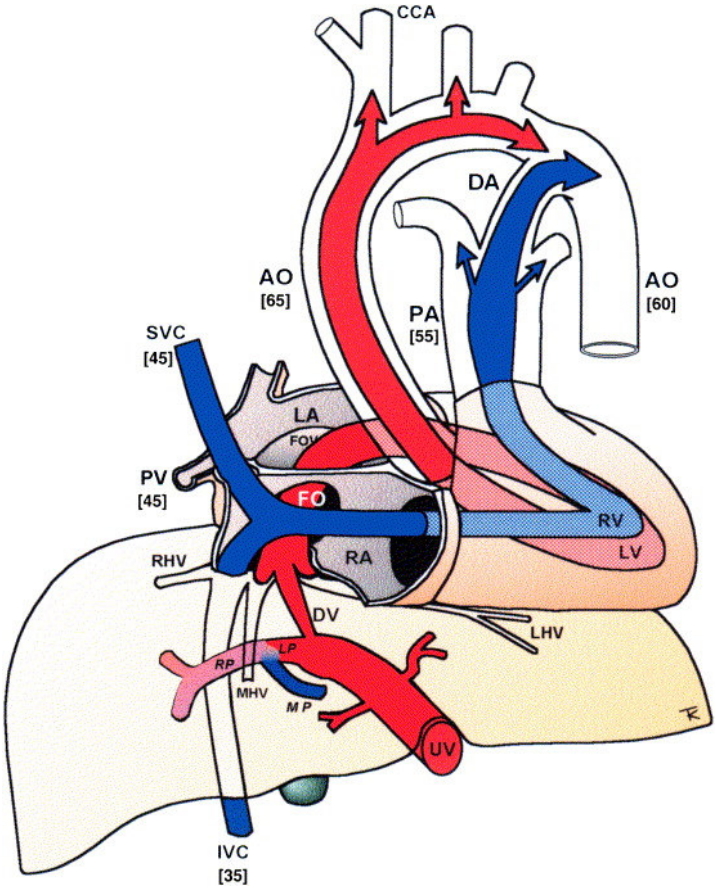

Figure 11. Graphic representation of the human fetal circulation. Oxygen saturation (%) of blood in different vessels is indicated in parenthesis. Umbilical vein (UV) has the most oxygenated (oxygen saturation ~85%) blood. CCA=common carotid artery, PA=pulmonary artery, RV = right ventricle, LV = left ventricle, SVC = superior vena cava, IVC =inferior vena cava, RA = right atrium, LA=left atrium, PV = pulmonary vein, FO = foramen ovale, DV = ductus venosus, RHV = right hepatic vein, MHV = middle hepatic vein, LHV = left hepatic vein, RP = right portal vein, LP= left portal vein, MP = main portal vein, DA = ductus aorteriosus, AO = aorta. The figure is reproduced with permission from Torvid Kiserud. *Seminars in Fetal and Neonatal Medicine*, 2005;10:493-503.

Fetal blood circulation differs from the postnatal circulation in several aspects (Rudolph, 1985; Kiserud & Acharya, 2004; Kiserud, 2005; Acharya et al, 2006). Fetal heart chambers function in parallel fashion compared to the serial arrangement postnatally and the intra-atrial and intra-ventricular pressures on the left and right sides are similar (Johnson et al, 2000). The heart rate of the fetus is two times faster than that of the adult. Right ventricle pumps blood to the pulmonary arteries, but the main portion of the ejected blood volume is

directed via the ductus arteriosus and the descending aorta to the lower body and placenta. Left ventricle pumps blood to the coronary circulation, upper body and brain.

Cardiac output

The stroke volume and cardiac output are positively associated with the gestational age. The stroke volume of the right ventricle has been reported to increase from 0.7 ml at 20 weeks to 7.6 ml at 40 weeks, whereas the stroke volume of the left ventricle increases from 0.7 ml to 5.2 ml during the same period (Kenny et al, 1986). There is a 10-fold increase in fetal cardiac output during the second half of pregnancy (Kenny et al, 1986; Räsänen et al, 1996; Kiserud et al, 2006), but the weight-indexed combined cardiac output remains relatively constant, approximately 400 - 425 ml/min/kg fetal weight (Kiserud et al, 2006; Mielke & Benda, 2001). The right ventricle has a slightly larger output (57% of the CCO) than the left ventricle (43% of the CCO) at 20 and 30 weeks of gestation. At 38 weeks the RVCO contributes to 60% of CCO (Räsänen et al, 1996).

Blood volume

The fetal blood volume is about 10-12% of the body weight compared to 7-8% in adults (Brace, 1983). The placenta contains a large pool of blood which constitutes around half of the total blood volume in the second trimester, although this amount decreases to 20% as pregnancy advances to term (Barcroft, 1946). The feto-placental blood volume increases with gestational age and has been shown to range between 18.5 to 81.4 ml (a mean blood volume of 16.2±2.06 ml/100 g fetal weight) at 16 -22 weeks in previable human fetuses with a body weight of 130 – 464 g (Morris et al, 1974) which is in accordance with the reported circulating fetal blood volume of 110-115 ml/kg (Brace, 1983, Yao et al, 1969).

Blood pressure

Systolic pressure of 30 - 46 mmHg, diastolic pressure of 22 - 27 mmHg and the mean arterial pressure of 28 -35 mmHg was recorded in the carotid artery of 5 human fetuses weighing 104 – 225 g exteriorized via a hysterotomy during termination of pregnancy (Rudolph et al, 1971). A mean arterial blood pressure of 15.2 mmHg in the umbilical artery of 13 human fetuses was recorded invasively during fetoscopy at 18-21 weeks of gestation (Castle & Mackenzie et al, 1986). In 30 fetuses undergoing cordocentesis at 19 -39 weeks, the mean umbilical arterial pressure was found to increase from approximately 23 mmHg at mid-gestation to 37 mmHg at term (Weiner, 1995). The fetus has a systolic ventricular pressure of 15-20 mmHg at 16 – 18

weeks of gestation, which increases to 35-40 mmHg at 26 - 28 weeks and the end-diastolic pressure is about 1-5 mmHg at 16-18 weeks, which increases slightly to 5-14 mmHg at 26 -28 weeks (Johnson et al, 2000). Fetal blood pressure increases with gestational age. Recently, some investigators have attempted to estimate fetal arterial blood pressure non-invasively from simultaneously derived aortic blood flow and diameter waveform recordings applying the Womersley model in combination with two element Windkessel model (Struijk et al, 2008) and found a mean arterial pressure of 28 mmHg at 20 weeks and 45 mmHg at 40 weeks of gestation.

At 16 - 28 weeks, the mean pressure in the right atrium is 3.660 mmHg and in the left atrium 3.357 mmHg (Johnson et al, 2000). The umbilical venous pressure varies between 4.5 - 6.0 mmHg from 18 weeks of gestation to term (Ville et al, 1994; Weiner et al, 1989).

Vascular resistance

The total resistance to blood flow in the fetal circulation is determined by fetal systemic, pulmonary and placental vascular resistances. Vascular resistances in the main pulmonary artery, ductus arteriosus, pulmonary vascular bed, descending aorta with its branches, and placenta determine the right ventricular afterload. The left ventricular afterload is mainly determined by the resistance in the ascending aorta and brachio-cephalic circulation.

Oxygen saturation

Oxygen saturation of blood in different blood vessels during fetal life is shown in Figure 11. Fetus receives oxygen-saturated blood from the placenta via the umbilical vein. Part of it is directed through the ductus venosus, and left hepatic vein towards the inferior vena cava and right atrium and across the foramen ovale to the left atrium and to left ventricle via the mitral valve. The venous return from the lower body and viscera and from the upper body and brain has the most deoxygenated blood, which is drained to the right atrium by the inferior and superior vena cave and directed to the right ventricle via the tricuspid valve.

In contrast to the adult circulation, oxygenated UV blood in the fetus mixes with deoxygenated systemic venous blood at several locations, although preferential streaming of blood via the ductus venosus separates well-oxygenated and poorly oxygenated blood. To some extent, oxygenated umbilical venous blood mixes along its path with systemic venous return in the right atrium and pulmonary venous return in the left atrium and the oxygen saturation decreases. Via dextra delivers blood to the lungs via two pulmonary arteries and to the lower body and placenta via ductus arteriosus and descending aorta. Via sinistra first

serves blood to the upper body (fetal head including brain, neck and upper extremities) but part of this blood is directed to the descending aorta across the aortic isthmus. The difference in oxygen saturation between the right and left ventricle is about 10% and between ascending and descending aorta even smaller (about 5%).

Shunts

Ductus venosus

Ductus venosus is a trumpet like vessel connecting umbilical vein to the inferior vena cava directing highly oxygenated blood towards the heart. Due to the higher kinetic energy, blood through the DV is diverted to the left atrium via the foramen ovale without much mixing with the deoxygenated blood entering the right atrium via the superior and inferior vena cavae. The length of the vessel is 5mm at 18 weeks and 15mm at 34 weeks and the mean diameter of the inlet is 0.5mm at midgestaion hardly exceeding 2mm through the rest of pregnancy (Kiserud et al, 1994; Kiserud et al, 2000). In humans in normal pregnancies the ductus venosus shunt fraction is approximately 30% of the umbilical venous blood at 20 weeks and 20% after 30 weeks until term (Kiserud et al, 2000; Haugen et al, 2004; Bellotti et al, 2000).

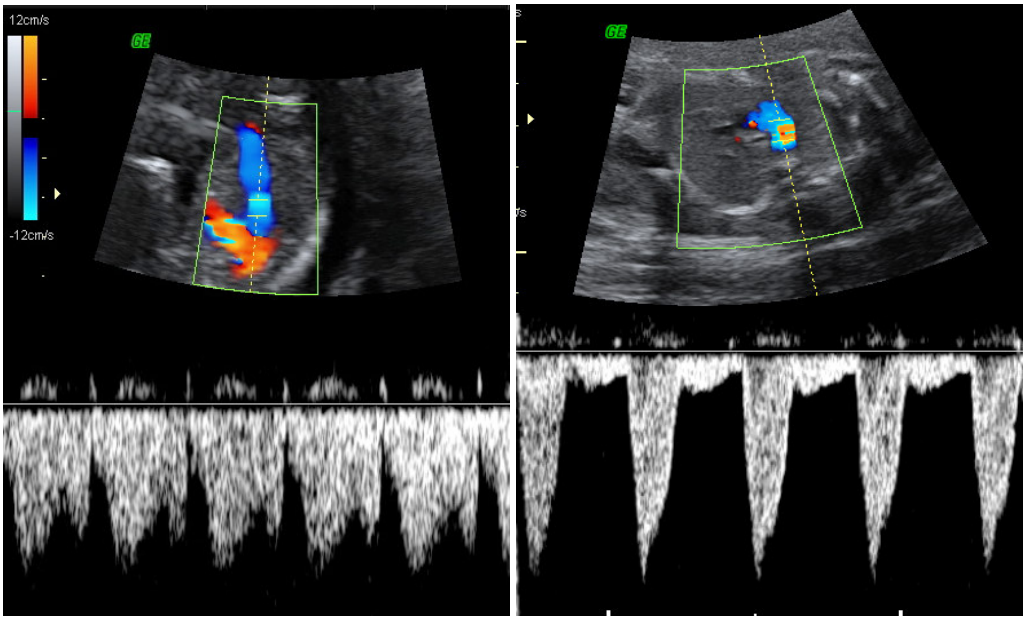

Figure 12. Colour directed and pulsed-wave Doppler recordings of ductus venosus blood flow (left) demonstrating the origin of ductus venosus (cursor) from the umbilical vein and typical flow velocity waveforms pattern at 12 weeks of gestation, and ductus arteriosus blood flow velocity waveforms (right) from a fetus at 18 weeks of gestation. *Figure by the courtesy of G. Acharya.*

Foramen ovale

Foramen ovale is a connection between the two atria and functions as a dividing crest between two atria directing most oxygenated blood to the left side of the heart. The diameter of the foramen ovale increases from 3 mm at 18 weeks to 6 mm at 32 weeks and remains relatively stable during the last part of pregnancy (Kiserud & Rasmussen, 2001). The volume blood flow through the foramen ovale is difficult to measure directly due to the difficulties associated with measuring the CSA and uncertain velocity profile of the multiphasic blood flow pattern (Phillipos et al, 1994; Räsänen at al, 1996). However, it can be calculated by subtracting the volume blood flow of the both pulmonary arteries from the LVCO and the fraction of CCO crossing the foramen ovale decreases from 34% at 18 weeks to about 18% at 30 weeks and beyond (Räsänen et al, 1996).

Ductus arteriosus

In the fetus, the ductus arteriosus is a large muscular vessel that connects pulmonary artery to the descending aorta. Prostaglandin E2 helps in maintaining its patency (Clyman et al, 1978). Normally 40-46% of the CCO is directed to the ductus arteriosus (Räsänen et al, 1996, Mielke & Benda, 2001), the amount diminishing after 30 weeks of the pregnancy while the pulmonary blood flow increases (Räsänen et al, 1996). The ductus arteriosus closes two days after birth (Huhta et al, 1984). The closure is triggered by the increase in arterial oxygen content (Coceani & Olley, 1988).

Watersheds

Aortic isthmus

Aortic isthmus is positioned in the arterial circulation, between left subclavian artery and the connection of ductus arteriosus to the descending aorta. It is an arterial “watershed” between upper body (incuding brain) and lower body (including placenta) circulations (Kiserud & Acharya, 2004, Kiserud 2005; Acharya et al, 2006; Acharya, 2009). Under physiological conditions there is antegrade flow of blood in the aortic isthmus during most of the cardiac cycle. During diastole when the semilunar valves are closed, the direction of blood flow in the aortic isthmus reflects solely the downstream impedances of the right and left ventricles (Fouron 2003). Increased lower body or placental impedance (Sonesson & Fouron, 1997) or decreased upperbody impedance (Patton & Fouron, 1995) cause an increase in retrograde blood flow component in human fetuses. Studies in fetal lamb suggest that hypooxygenation leads to increased blood flow reversal in the aortic isthmus (Mäkikallio et

al, 2006) and when the fetus is unable to maintain cerebral oxygenation the net aortic isthmus blood flow is reversed (Fouron et al, 1999). Aortic isthmus volume blood flow has not been measured in human fetuses.

Left portal vein

Fetal liver receives 80-86% of umbilical venous return of most oxygenated blood and the portal vein accounts for approximately 14-20 % of its venous blood supply in the second half of pregnancy (Kessler et al, 2008) with a fairly stable distribution of venous blood flow between the left (40%) and right (60%) lobes (Kessler et al, 2008; Haugen et al, 2004). The portal blood flow increases during the second half of pregnancy from 5 to 41 ml/min, and 10 to 13 ml/min/kg when normalized for estimated fetal weight (Kessler et al, 2007a).

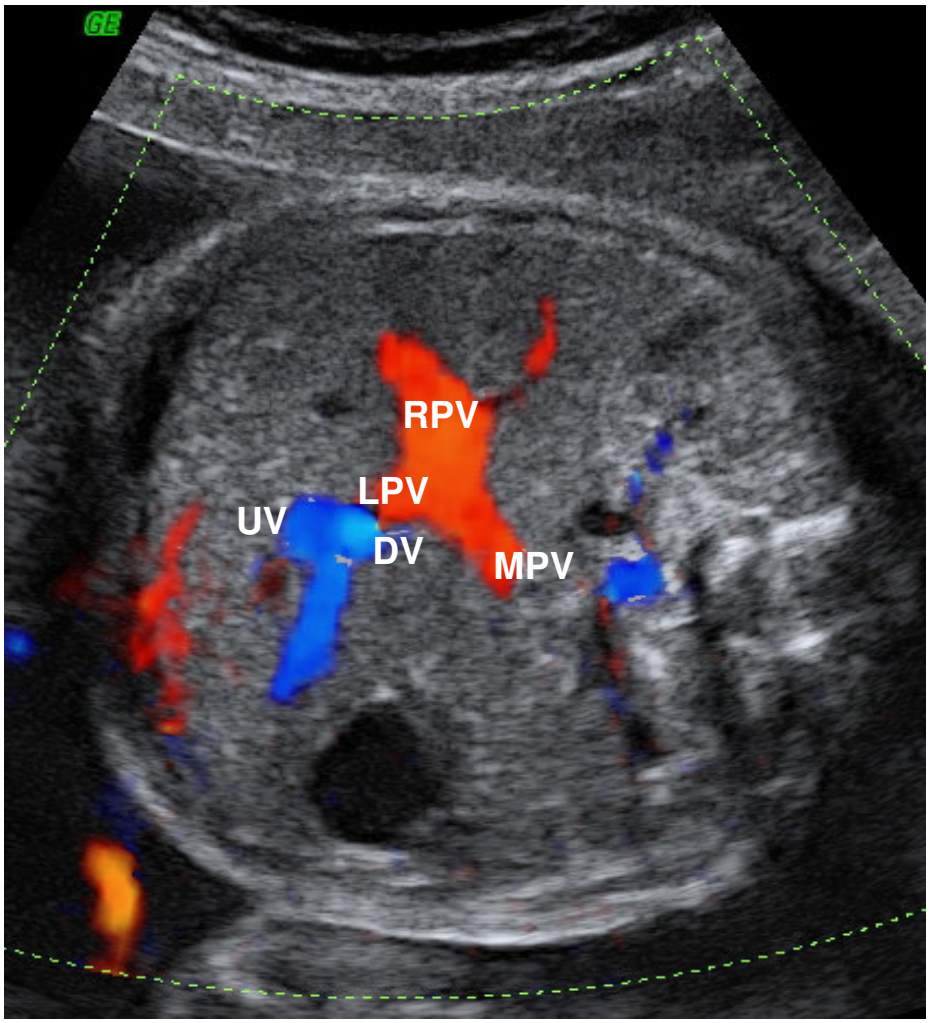

Figure 13. Colour Doppler (right) image of a cross-sectional view of the fetal abdomen demonstrating the umbilical vein (UV), left portal vein (LPV), ductus venosus (DV), right portal vein (RPV) and main portal vein (MPV). *Figure by the courtesy of G. Acharya.*

In the fetus, the left portal vein connects the umbilical vein with the portal circulation (splanchnic venous return) and is a venous "watershed" between umbilical (placental) and splanchnic (systemic) circulations (Kilavuz et al, 2003). Normally, umbilical venous blood supplies the left liver lobe and shunts a fraction of oxygenated blood to the ductus venosus first, before supplying the right liver lobe mixing with from the main portal vein. The direction of blood flow in the left portal vein reflects the relative balance between the umbilical venous pressure and portocaval pressure gradient. Blood flow in the left portal vein is generally orthograde towards the main portal stem and right liver lobe, but it may be reversed during fetal breathing (Kessler et al, 2007b). When the pressure in the umbilical vein is low, the ductus venosus shunt fraction increases but there may be cessation of umbilical venous blood flow to the left portal vein. In case of severe circulatory compromise, blood flow in the left portal vein may be reversed allowing splanchnic blood coming from the main portal stem to mix with the umbilical venous blood and enter the ductus venosus (Kiserud et al, 2003).

Placental circulation

Placenta is vital for the survival of the fetus, providing nutrition, oxygenation and waste exchange. It also has important endocrine, barrier and immunological functions. Placenta receives blood supply from the maternal and fetal side. On the maternal side about 83% of blood supply comes from two uterine arteries and 17 % from ovarian arteries (Wehrenberg et al, 1977). The fetal side of placenta is supplied by the two umbilical arteries. The mean volume blood flow to the placenta increases from 8.5 ml/min at 12 weeks to 80 ml/min at 28 weeks among fetuses weighing 90 to 650g (Assali et al, 1960) and is known to increase throughout the second half of gestation. Using non-invasive Doppler ultrasonography to measure umbilical vein blood flow longitudinally, it is reported to increase from 37 ml/min at 20 weeks to 263 ml/min at 40 weeks of gestation (Acharya et al, 2005a). Oxygenated blood returns from the placenta to the fetus via umbilical vein. The weight-indexed umbilical vein volume blood flow (Q_{uv}) has been reported to be 94 ml/kg/min at 12 weeks of gestation increasing to 123 ml/Kg/min at 26 weeks (Assali et al, 1960), and 90 ml/kg/min near term (Konje et al, 1996) using invasive (electromagnetic flow probe and ultrasonic transit-time flow probe, respectively) measurement techniques. A longitudinal study using Doppler ultrasonography in the second half of pregancy showed that the weight-indexed volume blood flow to the fetus increases to its maximum (117 ml/min/kg) at the end of second trimester and

thereafter decreases throughout the third trimester to approximately 66 ml/min/kg at 40 weeks (Acharya et al, 2005).

Placental vasculature has no neural regulation and catecholamines have little effect on the placental vessels. Endothelin and prostanoids have a vasoconstrictive effect (Poston, 1997) and nitric oxide has vasodilatory effect (Sand et al, 2002). The placental blood flow has been found to be stable and is mainly determined by fetal arterial blood pressure (Rudolph, 1985). The blood flow velocity waveforms recorded by Doppler in the umbilical artery, reflect the down stream impedance of the placental vasculature (Alfirevic & Neilson, 1995). The UA mean velocity increases and the pulsatility index decreases throughout the gestation (Mäkikallio et al, 2004; Acharya et al, 2005b; Acharya et al, 2005c). In the embryonic period the diastolic blood flow component is absent (Wloch et al, 2007) but becomes apparent after 12 weeks (Wladimiroff et al, 1991). A significant decrease in the number of small muscular arteries in the placental tertiary villi is associated with abnormal UA blood flow velocity waveforms (Giles et al, 1985).

Cerebral circulation

The fetal brain is supplied by two carotid and two vertebral arteries. Branches of these arteries supplying the brain are interconnected at the base of the skull to form a vascular ring, the circle of Willis (Figure 14). The venous return from the brain and upper body enters the heart via the superior vena cava. Most of the superior vena cava blood is directed to the right ventricle through the tricuspid valve via the right atrium.

In adult human, brain receives about 15% of the cardiac output and approximately 50 ml/min/100g tissue (Kety, 1950; Harper, 1965; Vavilala et al, 2002). In exteriorised human fetuses at 10-20 weeks gestation, the average fraction of CCO distributed to the brain was reported to be 14% and the mean blood flow was approximately 25ml/min/100g brain tissue among fetuses weighing 64-225g (Rudolph et al, 1971).

The brain blood flow is regulated by several homeostatic mechanisms and is significantly influenced by metabolic activity, PCO_2, PO_2, blood viscosity, and blood pressure (cerebral perfusion pressure). Relatively low oxygen tension and higher PCO_2 of the fetal blood may facilitate cerebral blood flow by reducing cerebrovascular resistance (Lucas et al, 1966). However, under normal conditions, between wide ranges of perfusion pressure, the cerebral blood flow is maintained constant by autoregulation. Unique features of cerebral circulation provide brain with stable blood flow, oxygen and substrate delivery, biochemical composition and temperature during hemodynamic, metabolic and thermal stresses.

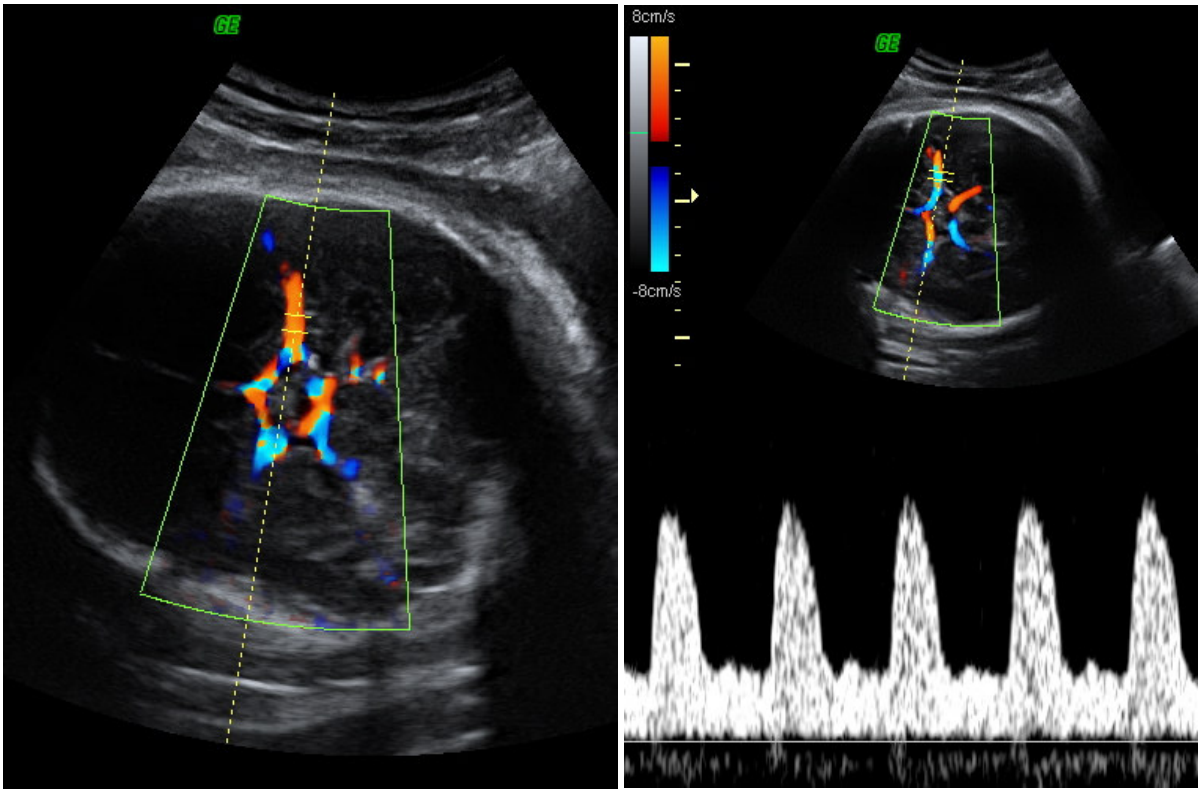

Figure 14. Colour Doppler image of the circle of Willis (left) demonstrating the middle cerebral artery (the Doppler sample volume is positioned at its proximal part) and the corresponding typical blood flow velocity waveforms (right lower panel). *Figure by the courtesy of G. Acharya.*

Distribution of cardiac output

Fetal cardiac output is significantly higher than that of the adult (Severi et al, 2000). The high cardiac output in the fetus is mainly due to the higher heart rate and central shunting that allows ventricles to work in parallel rather than in series. The fetal cardiac output increases with advancing gestation (Räsänen et al, 1996, Mielke & Brenda, 2001, Kiserud et al, 2006). The weight-indexed CCO is reported to be 363 (range, 175 – 660) ml/min/kg (although this is likely to be an underestimation as the pulmonary venous return was excluded from the calculation) among fetuses weighing 64 – 225g during the first half of pregnancy (Rudolph et al, 1971) and approximately, 400-425 ml/min/kg during the second half of pregnancy (Kiserud et al, 2006, Mielke & Benda 2001).

In the fetus, due to the parallel arrangement of circulation, blood distributed to various organs and placenta is derived from the systemic as well as the umbilical venous return (Rudolph, 2009). The outputs of the two ventricles are different with a clear right

ventricular dominance (Räsänen et al, 1996, Mielke & Benda, 2001, Kiserud et al, 2006) and blood to many organs is derived from both ventricles. The distribution of cardiac output varies with gestational age. Cardiac output distributed to the placenta in human pregnancies has been reported to increase during the first half of pregnancy. Using radionuclide-labelled microspheres in previable fetuses during legal abortion at 10-20 weeks of gestation, the fraction of CCO distributed to the placenta has been reported increase from 17% in fetuses weighing less than 50g to 33% in fetuses over 150g (Rudolph et al, 1971). Using non-invasive Doppler ultrasonography in the second half of pregnancy, this fraction has been shown to decrease from an average of 32% at 20 weeks to 21% after after 32 weeks of gestation (Kiserud et al, 2006).

In human fetuses, the fraction of CCO distributed to the lungs increases from 13% at 20 weeks to 25% at 30 weeks, decreasing thereafter to 21% at term (Räsänen et al, 1996). Another study estimated the pulmonary fraction of CCO to be 11% irrespective of gestational age (Mielke & Benda 2001). However, the distribution of RVCO is affected significantly by pulmonary vascular impedance, which is known to decrease 1.5-fold between 20 and 30 weeks of gestation and increase significantly thereafter (Räsänen et al, 1996). Hypoxia causes vasoconstriction (Lewis et al, 1976) and hyperoxia causes vasodilatation (Räsänen et al, 1998) of the pulmonary vasculature.

Due to large inter-species differences regarding the brain size relative to body size, it is most unreliable to extrapolate the finding from animal studies to human fetuses regarding the fraction of cardiac output distributed to the brain under physiological conditions. However, experimental studies have clearly provided useful information on relative changes in the distribution of blood flow that occur under pathological conditions (Jensen et al, 1999). Fraction of cardiac output distributed to the brain in human fetuses under physiological conditions is not known. A study on exteriorized fetuses during therapeutic abortion at 10-20 weeks reported this fraction to be approximately 14% (Rudolph et al, 1971).

The human fetus has different mechanisms to adjust its cerebral blood flow under different requirements. In acute hypoxia, the main mechanism is vasodilatation mediated by adenosine (it also diminishes oxygen consumption in neural tissues), nitric oxide and opioids. In chronic hypoxia, vasodilation resolves and energy conservation is prioritized (Pearce, 2006). The fetus can increase vascular resistance to diminish the brain blood flow if the oxygen availability is increased (Almstrom & Sonesson, 1996).

Oxygen delivery and consumption

Major function of the heart is to pump blood to maintain adequate perfusion of the organs and tissue to meet their metabolic demand. High metabolic demand of the growing fetal tissue is maintained by high blood flow rates and efficient oxygen extraction.

Analysis of blood samples obtained by cordocentesis from 208 normally grown fetuses has shown that the umbilical arterial and venous PO_2 (from 35.4 to 45.8 mmHg and from 32.6 to 37.6 mmHg, respectively), oxygen saturation (from 70 to 62% and from 90 to 75%, respectively) and pH (from 7.400 to 7.352 and 7.430 to 7.385, respectively) decrease, PCO_2 increases (from 35.4 to 45.8 and 32.6 to 37.6 mmHg, respectively) and the lactate values remain relatively stable (approximately, 0.92 mmol/l and 0.99 mmol/l, respectively) during 18 -38 weeks (Nicolaides et al, 1989). The decrease in PO_2 in UV blood with advancing gestational age is compensated by increasing hemoglobin concentration (from 10.8 to 14.5 g/dl) to keep the oxygen content relatively constant at approximately 6.0-6.7 mmol/l (Nicolaides et al, 1989; Soothill et al, 1986).

The oxygen consumption of the pregnant human uterus is reported to increase from 4.8 ml/min at 10 weeks to 22 ml/min at 28 weeks using electromagnetic flow probe to record the uterine blood flow (Assali et al, 1960) and at term it is reported to be on average 24.5 ± 12.7 ml/min using Fick principle (Metcalfe et al, 1955). Uterine oxygen consumption decreases to almost half following delivery (Assali et al, 1953) which suggests that the feto-placental unit is the main source of uterine oxygen consumption. The oxygen consumption of the human feto- placental unit is reported to be approximately 10.7 ml/min/kg (Bonds et al, 1986). Fetal oxygen consumption is a product of Q_{uv} and the difference in umbilical venous and arterial blood oxygen content. Oxygen consumption of the normal human fetus at 14 to 28 weeks of gestation varies between 3.0-5.4 ml/min/kg (Assali et al, 1960) and is approximately 6.6-6.8 ml/min/kg at term (Bonds et al, 1986; Acharya & Sitras, 2009). This value is higher than the consumption of the adult at rest, which is approximately 3.5 ml/min/kg (Dehmer et al, 1982). When oxygen consumption is increased (e.g. due to stress, infection etc.) the fetus may increase cardiac output (for example by increasing its heart rate) to ensure that the demand is met. When supply fails to meet demand despite maximal oxygen extraction from blood, anaerobic metabolism and lactic acidosis may occur.

ULTRASONOGRAPHY

Gray scale ultrasound

Ultrasound has 500-1000 times higher frequency than the audible sound. Much of the information used to generate an ultrasound image is based on the precise measurement of time. The time, an ultrasound pulse is transmitted and an echo is returned, is measured and the depth of the interface that generated the echo can be calculated when the propagation velocity of sound in the tissue is known according to the equation: *Distance (D) = ct/2*, where *c* = speed of the sound through the tissue and *t* = trip time, i.e. the total time taken by the ultrasound signal to travel to the tissue and return back to the transducer. Assuming constant ((~1540 m/s) propagation speed of sound in soft tissues; *D* (in mm) = *0.77*t* (in ms).

The conventional brightness-mode (B-mode) ultrasound imaging uses pulse-echo transmission, detection, and display techniques. Brief pulses of ultrasound energy are emitted by the transducer. When ultrasound is reflected, the signal contains amplitude, phase and frequency information. B-mode ultrasound uses amplitude information to generate the image in varying shades of gray (the brightness of the dots displayed on the two-dimensional image is proportional to the amplitude of the returning echoes from the tissues).

Different tissues have different acoustic impedance, meaning that the ultrasound travels in different speed in different tissues. Acoustic impedance is determined by the density of the tissue and the propagation velocity of sound in the tissue. Part of the ultrasound is reflected and refracted as does light in different interfaces. As the acoustic energy passes through tissue it is also attenuated. Acoustic power means the amount of acoustic pressure energy produced in a unit of time and acoustic intensity means the spatial distribution of power. Attenuation depends on the frequency as well on the tissue. Higher frequencies are attenuated more rapidly than lower frequencies.

The transducer works as a transmitter of ultrasound and a receiver of the reflected sound waves. The transmitting units send and receive in sequence. Controlling the time and sequence the units are fired, the ultrasound can be steered in different directions as well focused at different depths. High frequency transducers give better resolution but less penetration.

Spatial resolution

Spatial resolution refers to the ability of the ultrasound to detect and display structures that are anatomically separate. The axial resolution (along the beam axis) depends on the length of the

pulses used to form the ultrasound beam (spatial pulse length, SPL), i.e. *axial resolution* = *SPL/2*. The SPL is calculated from the wavelength (λ) and number of cycles within the pulse (n) as: $SPL=\lambda n$. Generally n is determined by the manufacturer (usually 2 - 4) and cannot be altered by the user. However, as λ is related to frequency (f) and propagation velocity (c) of sound ($\lambda=c/f$), spatial resolution can be improved by altering the wavelength by increasing the frequency of the transducer. Assuming that the pulse consists of 2 cycles (n = 2) and c = 1540, the axial resolution of a 5MHz transducer can be calculated to be: 0.31mm. Some advanced ultrasound systems have managed to almost double the axial resolution for a given transducer frequency by applying newer technologies, such as coded excitation to ultrasound imaging. Lateral resolution (perpendicular to the beam axis) equals to beam width and is controlled mainly by the number of transmitting elements. Lateral resolution can be improved by focusing the ultrasound beam to the region of interest. Therefore, best spatial resolution can be obtained by using the highest frequency of transducer that permits penetration to the depth of the region of interest and by optimizing the focal zone.

Doppler ultrasonography

When a moving target sends back an ultrasound wave, the reflected wave has a different frequency from the original. The frequency of the reflected waves is lower than the original if the target moves away from the transducer and vice versa. This Doppler phenomenon can be used to measure the properties of a moving target, e.g. velocity and direction of moving blood cells. The velocity of a moving target can be calculated by measuring the Doppler frequency shift as follows:

$V = (f_d * c)/(2 f_0 * \text{Cos}\theta)$, where c = velocity of sound, F_0 = initial (transducer) frequency, θ = angle of insonation, and F_d = Doppler frequency shift.

The angle of insonation has an impact on the velocity measured. An angle of zero degrees gives ($\text{Cos}0° = 1$) the ideal measurement. Whenever this cannot be achieved, angle correction should be used. However, an erroneous angle correction of 30° may introduce 13% error in velocity measurement ($\text{Cos}60° = 0.87$) and an angle of 60°, an error of 50% ($\text{Cos}30° = 0.5$). Therefore, for reasonably accurate velocity measurement, the angle of insonation should be kept <30°.

Pulsed-wave Doppler is usually used for blood flow measurements. This allows sampling from selected depths, by processing signals that return to the transducer after precisely timed intervals. The flow of data can be controlled in terms of shape, depth, phase

shift and position. The direction of blood flow can be displayed with different colours for the flow towards and away from the transducer.

There are several sources of errors and artefact in Doppler imaging. Wall filters remove low frequency signals from moving blood vessel walls, and should be used properly, especially when measuring low velocity blood flow. The Doppler sample volume needs to be positioned correctly to obtain velocities from the desired segment of the vessel and the gate size (length of the sample volume) influences the velocities that are displayed. The pulse repetition frequency (PRF) determines the sampling rate. The maximum frequency that can be measured by pulsed-wave Doppler (Nyquist limit) equals to half the PRF. When the Nyquist limit is exceeded aliasing phenomenon (ambiguous display of velocities) occurs. This can be minimized by increasing the PRF, decreasing the transmitted frequency of ultrasound, or increasing the angle of insonation. A technique called high PRF uses more than one gate (multi-gating) on the image to analyse the flow (Rumack et al, 2008), but has a disadvantage of not knowing the exact location of the Doppler shift.

Safety

Current limits in the United States allow spatial-peak temporal-average intensities of 720 mW/cm^2. American institute of Ultrasound in Medicine (AIUM) passed a consensus report on potential bioeffects of diagnostic Ultrasound in 2008 (Abramowicz *et al*, 2008). Its main conclusions were:

1. Acoustic output from diagnostic ultrasound devices is sufficient to cause temperature elevations in fetal tissues. The temperature rise near bone increases with ossification development throughout gestation. Temperature elevations become greater from B-mode to colour Doppler to pulsed-wave Doppler.
2. The TI is an index of calculated or estimated temperature rise that correlates with temperature elevation (TIs is the thermal index for soft tissue and TIb for bone). Mechanical index (MI) expresses the relative risk of cavitation and streaming.
3. Ultrasound exposure that elevates fetal temperature by 4ºC above normal temperature for 5 minutes or more has potential to cause severe developmental defects. Using commercially available equipment, it is unlikely that such thermal effect would occur.
4. No congenital anomalies have been attributed to diagnostic ultrasound.
5. Transducer self-heating can occur especially with vaginal probe, but no data is available for fetal temperature rise.

Epidemiological studies have not shown any significant adverse effects of clinical ultrasonography on the human fetus (Salvesen & Eik-Nes, 1999) but the safety continues to be a concern (Salvesen & Lees, 2009). International guidelines emphasize on responsible use of technology using ALARA (As Low As Reasonably Achievable) principle (Barnett et al, 2000) and output display monitoring to keep the mechanical index (MI) and thermal index (TI) below 1.9 and TI below 1.5, respectively (Barnett & Maulik, 2001).

AIMS OF THE STUDY

The aim of this thesis was to investigate some aspects of the fetal cardiac structure and function in the first half of pregnancy. The specific objectives were to:

1. Evaluate the feasibility of obtaining standard two-dimensional echocardiographic views of the fetal heart during routine first trimester screening using transvaginal ultrasonography.
2. Construct reference ranges for the measurement of cardiac ventricles, their outflow tracts and cardiothoracic circumference ratio at 11+0 to 13+6 weeks of gestation.
3. Establish longitudinal reference ranges for the a blood flow velocities and diameters of the ventricular outlets and measure serial changes in fetal cardiac output during 11-20 weeks of gestation
4. Establish reference ranges for the placental volume blood flow and measure the fraction of fetal cardiac output distributed to the placenta at 11-20 weeks of gestation.
5. Establish longitudinal reference ranges for the aortic isthmus diameter, blood flow velocities and related indices at 11-20 weeks of gestation.
6. Investigate serial changes in aortic isthmus volume blood flow and fraction of fetal cardiac output distributed to the upper body and brain at 11-20 weeks of gestation.

MATERIAL AND METHODS

First trimester transvaginal fetal echocardiography: A feasibility study (paper I)

Design and setting

This was a cross-sectional study of an unselected pregnant population attending the Central Maternity Unit, Health Centre of Tampere, Finland for routine first trimester ultrasound screening.

A contraindication to transvaginal ultrasonography or an inability to perform measurements within allocated 20 minutes of examination time excluded participation. The study protocol

was reviewed and approved by the Tampere University Hospital Ethics Committee (R02109). All participating women gave written informed consent. All pregnancies were followed and the outcome was recorded.

Study population

A total of 584 viable intra-uterine fetuses with a crown-rump length (CRL) between 41 mm (11+0 weeks) and 78 mm (13+6 weeks) were included.

Ultrasound equipment

Hitachi EUB-6000 ultrasound system (Hitachi Medical Corporation, Tokyo, Japan) with a 5 – 7.5MHz vaginal transducer was used.

Ultrasound examination

All examinations were performed by a single investigator (T. V.). Each session lasted approximately 20 minutes. The mechanical and thermal indices were kept below 1.1 and 0.9, respectively. After confirming fetal viability, CRL and NT were measured. The visceral situs and position of the heart within the chest was confirmed. Circumferences of the fetal thorax and heart were measured.

The fetal heart structures were assessed and measured by obtaining the following standard echocardiographic views:

1. Four-chamber view of the heart was obtained showing equal size ventricles and atria, opening and closure of atrioventricular valves, crux of the heart and interventricular septum. Using cine loop facility the largest transverse diameters of both ventricles were measured in diastole.
2. Longitudinal view of the aorta demonstrating its origin from the left ventricle and continuity with the interventricular septum was obtained. The diameter of the aorta at valve level was measured in systole.
3. Longitudinal view of the pulmonary trunk arising from right ventricle was obtained and the diameter of the pulmonary artery at valve level was measured in systole.
4. Crossing of the aorta and pulmonary artery was demonstrated and the three-vessel (pulmonary artery, aorta and superior vena cava) view was obtained.
5. Longitudinal view of the aortic arch was identified with branching head and neck vessels.

6. The continuation of pulmonary trunk into the descending aorta (ductal arch) was demonstrated.

Fetal cardiac output and its distribution to the placenta and brain (paper II & III)

Design and setting

This was a prospective longitudinal study pregnant women recruited from an unselected population attending the Central Maternity Unit, Health Centre of Tampere, Finland for routine first trimester nuchal translucency (NT) screening. Exclusion criteria were multiple pregnancy, smoking and history of medical illness that might have a significant effect on the course of pregnancy.

The study protocol was reviewed and approved by the Tampere University Hospital Ethics Committee (R06108). All participating women gave written informed consent. All pregnancies were followed and the outcome was recorded.

Study population

A total of 143 healthy pregnant women with singleton pregnancies and an uncomplicated obstetric history were included.

Ultrasound equipment

A Voluson 730 Expert (GE Medical Systems, Kretz Ultrasound, Zipf, Austria) ultrasound system equipped with RICS5-9H vaginal and RAB4-8L abdominal transducers was used.

Ultrasound examination

A single investigator (T. V.) performed all examinations. First examination was performed using a transvaginal probe at 11+0 - 13+6 weeks of gestation and subsequent examinations were performed transabdominally at approximately three-weekly intervals. Each session lasted a maximum of 30 minutes. The ALARA principle was applied and the MI and TI were kept below 1.5 and 1.9, respectively at all times. Biparietal diameter (BPD), head circumference (HC), abdominal circumference (AC) and femur length (FL) were measured on each visit and fetal weight was estimated using the Hadlock-1 equation. After routine survey of fetal anatomy, standard views of the fetal heart were obtained to confirm normality. Colour Doppler was used to identify and visualize the direction of blood flow. Blood flow velocity waveforms were obtained using pulsed-wave Doppler.

Measurement of umbilical vein volume blood flow

Umbilical vein Doppler velocity waveform and inner diameter of the vessel were measured at the intra-abdominal straight portion (Figure 15). The blood flow velocity waveforms were recorded for 2-4 s and time-averaged maximum velocity (TAMXV) was measured. The umbilical vein volume blood flow (Q_{uv}) was calculated as: Q_{uv} (ml/min) = π * (diameter in cm/2)^2 * 0.5 * TAMXV in cm/s * 60 assuming a parabolic velocity profile (Acharya et al, 2005, Kiserud et al, 2000) and circular cross-section of the vessel.

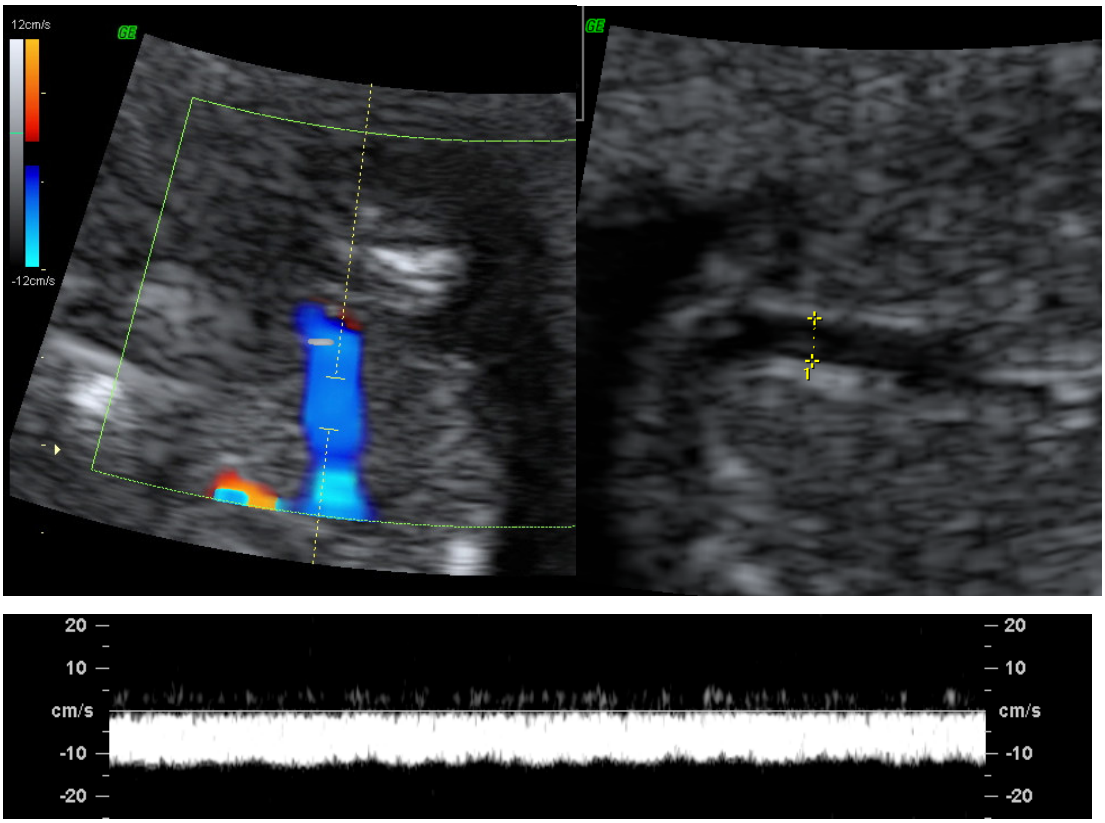

Figure 15. Measurement of blood velocity (left) and diameter (right) of the umbilical vein at the intra-abdominal straight portion in a fetus at 13 weeks of gestation. The blood flow velocity waveform is displayed in the lower panel.

Measurement of fetal cardiac output

The inner diameters of the aorta and pulmonary artery were measured at the valve level in systole. The cine loop facility was used to identify systole. An average of three separate measurements was used for statistical analysis (Kiserud & Rasmussen, 1998).

Doppler velocity waveforms were obtained from the aorta and pulmonary artery at the valve level. The angle of insonation was kept as low as possible and angle correction

was used when required. Blood flow velocity waveforms were recorded for 2-4 s during fetal quiescence. Three representative heart cycles were traced for the measurement of velocity time integral (VTI) and fetal heart rate (FHR). The TAMXV was calculated as the product of VTI and FHR. The volume blood flow (Q) through the aorta (LVCO) and the pulmonary artery (RVCO) was calculated separately as: $Q\ (ml/min) = \pi * (diameter/2)^2 * TAMXV\ in\ cm/s * 60$ assuming a flat velocity profile, i.e. velocity profile coefficient, $h = 1$. The combined cardiac output (CCO) was obtained by summing the LVCO and RVCO.

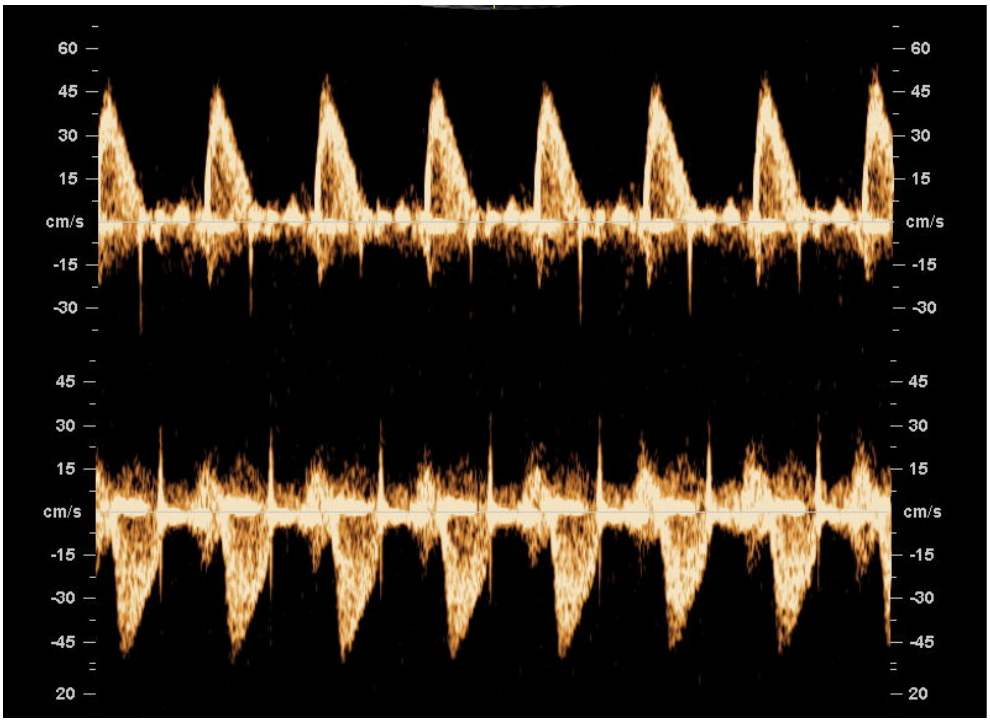

Figure 16. Blood flow velocity waveforms obtained from the aortic valve (top panel) and pulmonary valve (lower panel) of a fetus at 13 weeks of gestation.

Measurement of aortic isthmus blood flow

Doppler velocity waveforms were obtained from the aortic isthmus (AI) during fetal quiescence. The angle of insonation was kept as low as possible and angle correction was used as required. The inner diameter of AI was measured just after the origin of left subclavian artery in systole, and an average of three measurements was recorded. The cine loop facility was used to identify systole. Three representative heart cycles were traced for TAMXV and the average was used for volume blood flow (Q_{ai}) calculations. The Q_{ai} was calculated as: $Q_{ai}\ (ml/min) = \pi * (diameter\ in\ cm/2)^2 * TAMXV\ in\ cm/s * 60.$

The pulsatility index (PI) and resistance index (RI) of the AI were calculated as (peak systolic velocity – end-diastolic velocity)/ TAMXV and (peak systolic velocity – end-diastolic velocity)/ peak systolic velocity, respectively.

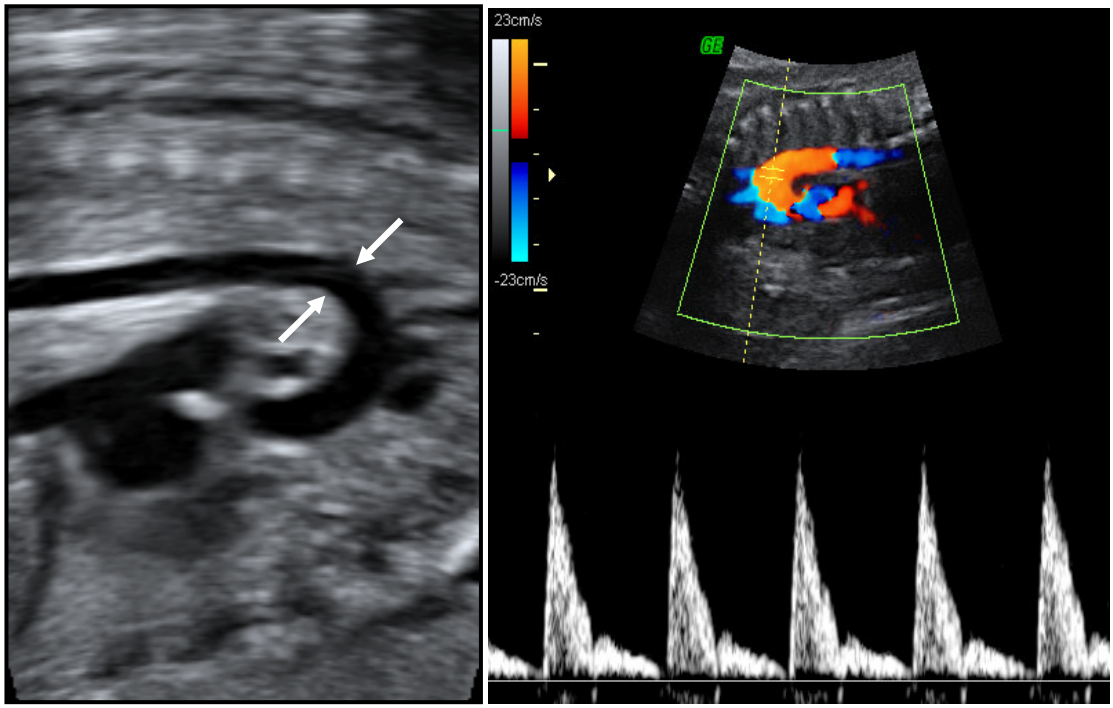

Figure 17. Measurement of aortic isthmus diameter (between the arrows) using B-mode ultrasonography distal of the exit of left subclavian artery and blood flow velocities using colour directed pulsed-wave Doppler in a fetus at 16 weeks of gestation.

Distribution of cardiac output

The placental fraction of the CCO was calculated as: Q_{uv}/CCO * 100. The fraction of CCO distributed to the upper body and brain calculated as: (LVCO-Q_{ai})/CCO * 100, without accounting for the coronary blood flow.

Reproducibility

Intra-observer reproducibility was studied in 20 separate fetuses at 11-13 weeks and 18-20 weeks of gestation. As all the measurements were performed by a single investigator using same ultrasound equipment, we calculated intraclass correlation coefficient (ICC) and repeatability coefficient with their 95% confidence intervals (Bartlett & Frost, 2008) to assess the reproducibility.

Statistical analysis

Power calculation for the study I was performed assuming that approximately 20 observations per gestational day are required to construct reliable reference intervals. For a total of 21 days between 11+0 and 13+6 weeks the required number of observation was 420. Assuming a success rate of 60% for visualising the cardiac structures and obtaining reliable measurements, we calculated this number to be 588. Adding 23 more observations to account for dropouts and loss of follow-up we estimated a sample size of 611 fetuses.

Cross-sectional data from the study I were analyzed using Statistical Package for Social Sciences for Windows version 14.0 (SPSS Inc., Chicago, IL, USA). Assumption of normality was checked and data transformation was performed as required to achieve normal distribution. Reference percentiles were calculated according to the method described by Royston & Wright (1998).

For study II & III, power calculation was performed assuming that if approximately 20 observations per gestational week are required to construct reliable reference ranges in a cross-sectional study (i.e. 200 observations/participants for a period of 10 weeks between 11 and 20 gestational weeks), the corresponding number of participants for a longitudinal study would be 200/2.3 (i.e. 87), where 2.3 is a design factor (Royston & Altmann, 1995). With a believe that it would be possible to obtain the desired measurements in at least 60% of cases, we calculated a sample size of 122 and added 21 extra to account for possible dropouts giving a total number of 143 participants.

The longitudinal data were analyzed using SAS 9.0 (SAS Institute Inc., Cary, NC, USA). Assumption of normality was checked for each variable. Logarithmic or power transformations were performed as appropriate. The best transformation was obtained using Box-Cox regression. Fractional polynomials were used to obtain best fitting curves in relation to gestational age for each outcome variable analyzed. Multilevel modelling was used to estimate the reference percentiles (Royston, 1995).

RESULTS

General characteristics of the study population

In study I, a total of 599 women were enrolled and 611 fetuses were studied. CRL and/or NT was not possible to measure from 22 fetuses, leaving 584 for final analysis. In study II and III 143 women enrolled the study and total of 424 observations were made. The basic characteristics of the two study populations are described in table 1.

Table 1. Characteristics of the study populations

	Age, years	BMI Kg/m^2	Nulliparous	Caesarean section rate	Neonatal birth weight, g	5min. Apgar score <7
Study 1	28 (15-44)	25 (17-44)	50 %	13 %	3510	8
Study II & III	29 (17-39)	24.5 (19-38)	51 %	13 %	3540	0

Success rate of ultrasound examination

Study I was performed to study the feasibility of the first trimester echocardiography in an unselected population. The success rate of complete visualization of different cardiac structures at gestational ages 11+0 to 13+6 ranged between 43 to 62%.

In study 1, there were six cardiac malformations. One atrioventricular septal defect was diagnosed at 13 weeks. The karyotype was normal, but the fetus developed hydrops and died at 16 weeks of gestation. One fetus had hypoplastic left heart syndrome. Four-chamber view was not satisfactory at 13 weeks, NT was 3.1mm, and karyotype was normal. Follow-up examination at 18 weeks of gestation confirmed the diagnosis and the mother opted for termination of pregnancy. Four fetuses had ventricular septal defects, but none were diagnosed prenatally. One of the babies with ventricular septal defect had Goldenhair syndrome, the defect was subvalvular and was surgically closed at 5 months of age. The other three defects were in the muscular part of the septum and they closed spontaneously before one year of age.

In study II & III there were total of 424 observations. Table 2 presents the success rates of acquiring the volume blood flows at different gestational ages.

Table 2. Success rates (%) of acquiring combined cardiac output (CCO) and aortic isthmus volume blood flow (Q_{ai}) at different gestational ages

Gestational age, weeks+days	11+0 - 13+6	14+0 -16+6	17+0 - 20+6
study II (CCO)	46	61	71
study III (Q_{ai})	33	62	82

Reference values

Study I

We have established reference ranges for fetal heart left and right ventricular diameter, aorta and pulmonary artery diameter at the valve level and cardio-thoracic ratio in late first trimester.

Study II

Reference percentiles for the diameter of the aorta, pulmonary artery, and intra-abdominal portion of the umbilical vein are presented in Tables 3, 4 and 5, respectively. The TAMXV of the aorta, pulmonary artery and umbilical vein are presented in Tables 6, 7 and 8, respectively. Vessel diameters and blood flow velocities increased with advancing gestation. Reference ranges were established for the LVCO, RVCO, CCO, weight-indexed CCO, $Q_{uv,}$ weight-indexed Q_{uv} and fraction of CCO distributed to the placenta during 11-20 weeks of gestation. The CCO increased from 9 ml/min to 121 ml/min and Q_{uv} from 1.9 ml/min to 25.3 ml/min during 11-20 weeks of gestation. The weight-indexed combined cardiac output increased during 11-20 weeks from 183 ml/min/kg to 342 ml/min/kg, i.e. almost doubled. The weight-indexed umbilical vein volume flow increased from 24 ml/min/kg to 71 ml/min/kg, i.e. a 3-fold increase. Fetus directs 14% of CCO to the placenta at 11 weeks of gestation and 21% at 20 weeks.

Table 3. Reference intervals for the aortic diameter at the semilunar valve level (cm)

Gestation, weeks	2.5th centile	5th centile	10th centile	25th centile	50th centile	75th centile	90th centile	95th centile	97.5th centile
11	0.06	0.07	0.07	0.08	0.10	0.11	0.12	0.13	0.14
12	0.08	0.08	0.09	0.10	0.11	0.12	0.13	0.14	0.15
13	0.09	0.10	0.10	0.11	0.12	0.14	0.15	0.16	0.17
14	0.11	0.11	0.12	0.13	0.15	0.16	0.17	0.18	0.19
15	0.12	0.13	0.14	0.15	0.16	0.18	0.19	0.20	0.21
16	0.14	0.15	0.16	0.17	0.18	0.20	0.21	0.22	0.23
17	0.16	0.17	0.18	0.19	0.20	0.22	0.24	0.24	0.25
18	0.18	0.19	0.20	0.21	0.23	0.25	0.26	0.27	0.28
19	0.21	0.21	0.22	0.24	0.25	0.27	0.29	0.30	0.31
20	0.23	0.24	0.25	0.26	0.28	0.30	0.32	0.33	0.34

Table 4. Reference intervals for the pulmonary artery diameter at the semilunar valve level (cm)

Gestation, weeks	2.5th centile	5th centile	10th centile	25th centile	50th centile	75th centile	90th centile	95th centile	97.5th centile
11	0.07	0.07	0.08	0.09	0.10	0.11	0.13	0.13	0.14
12	0.08	0.08	0.09	0.10	0.11	0.13	0.14	0.15	0.15
13	0.09	0.10	0.10	0.12	0.13	0.14	0.16	0.16	0.17
14	0.11	0.12	0.12	0.14	0.15	0.16	0.18	0.19	0.19
15	0.13	0.13	0.14	0.15	0.17	0.18	0.19	0.20	0.21
16	0.15	0.15	0.16	0.17	0.19	0.20	0.22	0.23	0.23
17	0.17	0.17	0.18	0.19	0.21	0.22	0.24	0.25	0.26
18	0.19	0.20	0.20	0.22	0.23	0.25	0.27	0.28	0.29
19	0.21	0.22	0.23	0.24	0.26	0.28	0.30	0.31	0.32
20	0.24	0.24	0.25	0.27	0.29	0.31	0.33	0.34	0.35

Table 5. Reference intervals for the umbilical vein diameter at the intra-abdominal portion (cm)

Gestation, weeks	2.5th centile	5th centile	10th centile	25th centile	50th centile	75th centile	90th centile	95th centile	97.5th centile
11	0.07	0.07	0.08	0.09	0.10	0.11	0.12	0.12	0.13
12	0.08	0.08	0.09	0.10	0.11	0.12	0.13	0.14	0.14
13	0.09	0.10	0.10	0.11	0.12	0.13	0.15	0.15	0.16
14	0.11	0.11	0.12	0.13	0.14	0.15	0.16	0.17	0.18
15	0.12	0.13	0.13	0.14	0.16	0.17	0.18	0.19	0.20
16	0.14	0.15	0.15	0.16	0.18	0.19	0.20	0.21	0.22
17	0.16	0.16	0.17	0.18	0.20	0.21	0.23	0.23	0.24
18	0.18	0.18	0.19	0.20	0.22	0.23	0.25	0.26	0.27
19	0.20	0.20	0.21	0.23	0.24	0.26	0.27	0.28	0.29
20	0.22	0.23	0.23	0.25	0.27	0.28	0.30	0.31	0.32

Table 6. Reference ranges for the time-averaged maximum blood flow velocity of the aorta (cm/s)

Gestation, weeks	2.5th centile	5th centile	10th centile	25th centile	50th centile	75th centile	90th centile	95th centile	97.5th centile
11	5.7	6.1	6.6	7.5	8.5	9.7	10.8	11.6	12.3
12	6.6	7.0	7.5	8.5	9.6	10.9	12.1	12.9	13.7
13	7.4	7.9	8.4	9.5	10.7	12.1	13.4	14.3	15.1
14	8.2	8.7	9.3	10.4	11.8	13.2	14.7	15.6	16.4
15	8.8	9.3	9.9	11.1	12.4	14.0	15.5	16.4	17.3
16	9.3	9.8	10.5	11.7	13.1	14.7	16.3	17.3	18.2
17	9.7	10.3	11.0	12.2	13.7	15.4	17.0	18.0	18.9
18	10.1	10.7	11.4	12.7	14.3	15.9	17.6	18.6	19.6
19	10.5	11.1	11.8	13.1	14.7	16.4	18.1	19.2	20.2
20	10.8	11.4	12.2	13.5	15.1	16.9	18.6	19.7	20.7

Table 7. Reference ranges for the time-averaged maximum blood flow velocity of the pulmonary artery (cm/s)

Gestation, weeks	2.5th centile	5th centile	10th centile	25th centile	50th centile	75th centile	90th centile	95th centile	97.5th centile
11	6.8	7.2	7.6	8.4	9.4	10.5	11.6	12.3	12.9
12	7.6	8.0	8.5	9.4	10.5	11.7	12.8	13.6	14.3
13	8.5	8.9	9.4	10.4	11.6	12.8	14.1	14.9	15.6
14	9.3	9.8	10.4	11.4	12.6	14.0	15.3	16.2	17.0
15	9.8	10.3	10.9	12.0	13.3	14.7	16.1	17.0	17.9
16	10.4	10.9	11.5	12.6	14.0	15.5	17.0	17.9	18.7
17	10.8	11.4	12.0	13.2	14.6	16.1	17.7	18.6	19.5
18	11.2	11.8	12.5	13.7	15.1	16.7	18.3	19.3	20.2
19	11.6	12.2	12.9	14.1	15.6	17.2	18.8	19.8	20.7
20	11.9	12.5	13.2	14.5	16.0	17.6	19.3	20.3	21.2

Table 8. Reference ranges for the umbilical vein time-averaged maximum blood flow velocity (cm/s)

Gestation, weeks	2.5th centile	5th centile	10th centile	25th centile	50th centile	75th centile	90th centile	95th centile	97.5th centile
11	2.7	3.0	3.4	4.1	5.0	6.1	7.2	7.9	8.6
12	3.6	3.9	4.4	5.2	6.3	7.6	8.9	9.7	10.5
13	4.5	5.0	5.5	6.5	7.7	9.2	10.7	11.6	12.5
14	5.4	5.9	6.5	7.6	9.1	10.7	12.3	13.4	14.4
15	6.3	6.8	7.5	8.7	10.2	12.0	13.8	15.0	16.1
16	7.0	7.6	8.3	9.6	11.3	13.2	15.1	16.4	17.5
17	7.7	8.3	9.1	10.5	12.3	14.3	16.3	17.6	18.8
18	8.3	8.9	9.7	11.2	13.1	15.2	17.3	18.7	20.0
19	8.8	9.5	10.3	11.9	13.8	16.0	18.2	19.7	21.0
20	9.3	10.0	10.9	12.5	14.5	16.8	19.1	20.5	21.9

Study III

Reference ranges were established for the aortic isthmus blood flow velocities, vessel diameter, PI, RI, Q_{ai} and the fraction of CCO distributed to the upper body and brain. Aortic isthmus diameter increased linearly during 11-20 weeks of gestation. PSV, EDV and TAmax increased from 30-63 cm/s, 1.7-5.4 cm/s and 11.9-22.2 cm/s respectively during 11-20 weeks of gestation. RI and PI stayed fairly stable (0.94-0.91 and 2.38-2.62, respectively) during 11-20 weeks. Q_{ai} increased from 2.6 ml/min to 41.5 ml/min and the fraction from CCO delivered to the upper body was approximately 13%.

DISCUSSION

General considerations

This study was conducted with the main purpose of measuring the serial changes in fetal cardiac output and its distribution to the placenta and upper body including brain during 11-20 weeks of gestation under physiological conditions. At first we were compelled to explore the feasibility of performing fetal echocardiography recognising different structures and obtaining images of adequate quality to be able to measure the structures in the late first trimester (study I). The feasibility of performing fetal echocardiography to diagnose congenital heart defects in high-risk populations has been demonstrated previously by other investigators (Dolkart & Reimers, 1991; Gembruch et al, 1993; Gembruch et al, 2000; Haak et al, 2002; Johnson et al, 1992). We wished to do this in a non-selected population to create reference ranges for vessel diameter, especially for the aorta and pulmonary artery, which is required for the measurement of feta cardiac output. We also measured the ventricular diameters and the cardio-thoracic ratio, which is a useful measurement for evaluating heart function (Hofstaetter et al, 2006; Huhta, 2004; Mäkikallio et al, 2008), as cardiomegaly is a consistent feature of congestive heart failure. Doppler velocimetry was not performed in this cross-sectional study to minimize fetal exposure to ultrasound energy.

It was feasible to assess and measure fetal heart structures in approximately 2/3 of cases within the time frame used for routine nuchal translucency screening. Our success rate was slightly lower than reported in some previously published studies (Gembruch et al, 1993; Gembruch et al, 2000; Haak et al, 2002; Johnson et al, 1992; Dolkart & Reimers, 1991), which was perhaps due to the rigid time frame allowed for each examination. Although the consensus and recommendation to date is to perform routine screening echocardiography in the second trimester (IUSOG Statement Lee et al, 2008), our results indicate that it is

possible confirm normality in the late first trimester in a majority of cases. Therefore, a policy of performing fetal echocardiography in the first trimester in high-risk groups and if required, repeating in the second trimester to confirm the findings (Allan, 2003) may be reasonable. Study I gave valuable training in performing the measurements for study II & III. Although we did not collect data to measure the learning curve, but it can be speculated that the examinations became more successful as experience accumulated (Allan, 2006; Tegnander & Eik-Nes, 2006). Several studies have shown an increased incidence of cardiac malformations in fetuses with increased nuchal translucency (Haak et al, 2002; Makrydimas et al, 2003; Clur et al, 2008; McAuliffe et al, 2004; Hyett et al, 1997) and there may be a rationale for evaluating the fetal heart structure as well as function routinely during first trimester ultrasound screening.

Volume blood flows were measured in the aorta, pulmonary artery, aortic isthmus and umbilical vein to study serial changes in fetal cardiac output and its distribution to placenta and upper body including brain (Study II & III). We chose longitudinal design to establish reference ranges for serial measurements with advancing gestation. Temporal changes cannot be studied with cross-sectional design. Longitudinal reference ranges can be useful in clinical practice as Doppler parameters are often measured serially. Additionally, longitudinal data allow for the calculation of conditional reference intervals based on previous measurements (Royston, 1995).

The volume blood flow to the placenta has been previously examined noninvasively in human fetuses cross-sectionally (Sutton et al, 1990; Barbera et al, 1999; Kiserud et al, 2000) and longitudinally (Acharya et al, 2005a) in the second half of pregnancy. However, in the first half of pregnancy this has been measured only invasively in exteriorised human fetuses during termination of pregnancy by hysterotomy using radionucleotide microspheres (Rudolph et al, 1971). We provide Doppler derived reference ranges for the UV diameter, blood flow velocity and Q_{uv} during 11-20 weeks of gestation that may be useful for evaluating feto-placental circulation in the first half of pregnancy.

The weight-indexed CCO almost doubled (183 to 342 ml/min/kg) whereas the weight-indexed Q_{uv} tripled (24 to 71 ml/min/kg) during 11-20 weeks of gestation. The fraction of CCO delivered to placenta increased from 14 % to 21 % during the same gestational period whereas the fraction of CCO delivered to the upper body including brain was relatively constant at approximately 13%. Blood flow to an organ is usually a function of growth and metabolic activity. Placental growth is faster than the fetal growth during the second trimester whereas the opposite is true for the third trimester of pregnancy (Molteni et

al, 1978). Our finding of increased Q_{uv} normalized for estimated fetal weight during 11 to 20 weeks is consistent with this concept despite the insecurity of fetal weight estimation using ultrasound biometry during the first half of pregnancy.

Different organs of the fetus grow at different rates during pregnancy. Liver, heart, thyroid gland and brain appear to grow at a relatively constant rate. Brain constitutes about 15% of body weight in the human fetuses weighing 1-500g (Tanimura et al, 1971). Brain weight expressed as percentage of body weight shows essentially no change until birth and the main change occurs after birth with an absolute increase in brain mass of nearly 600g during the first year of life (Walsh et al, 1974). The rate of cerebral blood flow in the human fetus under physiological conditions is not known. Our finding of an almost constant fraction of CCO diverted to upper body and brain during 11-20 weeks fits well with the relatively constant growth of fetal brain during this period of gestation.

When the amount of blood flow directed to the upper body including brain and heart was subtracted from the LVCO we found that approximately $3/4^{th}$ of LVCO is diverted to the descending aorta during 11-20 weeks of gestation. A little less than 80% of RVCO reaches the descending aorta through the ductus arteriosus (Mielke & Benda, 2001). In this respect, the general concept that the left heart delivers blood to the upper body and brain and the right heart to the lungs, lower body and placenta may not be quite accurate. Right heart does deliver most of its output to the lower body and placenta, but the left ventricle also appears to contribute quite significantly, at least during 11-20 weeks gestation, under physiological conditions. The fetal heart has been shown to have right ventricular dominance in the second half of the pregnancy and it increases as the gestation progresses (Räsänen et al, 1996). We found the right heart dominance to be present also at 11-20 weeks of gestation but it decreased from 13% at 11 weeks to 8% at 20 weeks of gestation.

Placental volume blood flow is shown to be reduced earlier than demonstrable changes in umbilical artery Doppler waveform pattern (Ferrazi et al, 2002) and the fraction of fetal CCO distributed to the placenta is lower in intrauterine growth restriction (Kiserud et al, 2006). Changes in aortic isthmus blood flow velocity indices seem to occur earlier than the changes in umbilical artery (Sonesson & Fouron, 1997) and ductus venosus (Rizzo et al, 2008; Figueras et al, 2009). Studying the distribution of fetal CCO to the placenta, upper body and brain by measuring volume blood flows may provide valuable information on fetal adaptive mechanisms related to suboptimal *in utero* conditions.

Methodological aspects and limitations

The position and the size of Doppler gate (sample volume) are operator controlled. A large sample volume increases the chance of covering the whole cross-section of the blood vessel and detecting all the velocities, but may result in sampling the adjacent vessels and spectral broadening. Additionally, one has no control over the lateral extension of the sample volume. To avoid this we adjusted the sample volume according to the size of blood vessel studied. The angle of insonation was kept as low as possible and angle correction was used when required while measuring the blood flow velocities.

To avoid variations in the velocity and diameter measurement we sampled the umbilical vein at the intra-abdominal portion rather than the free-loop of the umbilical cord. Furthermore, our intra-abdominal UV diameter measurements correspond well with the reported measurements performed on the pathological specimens (Malas et al, 2003). We used TAMXV and corrected it by the spatial velocity profile coefficient rather than using the time-averaged intensity weighted mean velocity (TAV) for the calculation of Q_{uv}. Use of TAV avoids the need for correction for the spatial velocity profile, but it is affected by machine settings, e.g. Doppler gain, wall filter etc. and is more software dependent. Although, the velocity profile of the umbilical vein varies along the length of the umbilical cord (Pennati et al, 2004), it is likely to be parabolic (has spatial velocity profile coefficient of 0.5) at the intra-abdominal portion (Acharya et al, 2005a).

Velocity and diameter measurements of the aorta and pulmonary artery were performed at the valve level, which is a clear anatomical landmark. While measuring the velocity and diameter of the aortic isthmus we chose longitudinal aortic arch view rather than the cross-sectional three-vessel view, as it is easier to indentify the origin of left subclavian artery in that view (Acharya, 2009) allowing accurate identification of aortic isthmus and calliper and cursor placement. Other physiological aspects of aortic isthmus blood flow waveform pattern (Figure 18) were taken into account to identify and ensure that the waveforms were not from adjacent vessels.

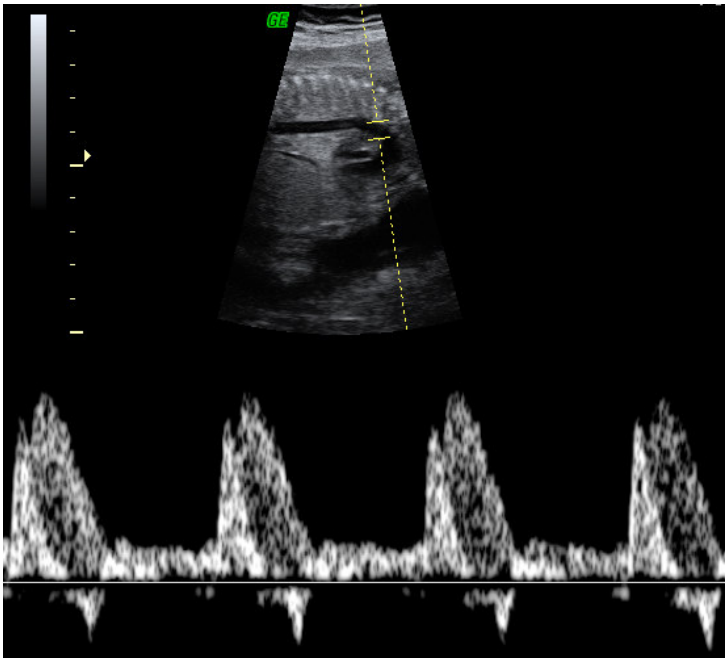

Figure 18. Doppler blood flow velocity waveforms recorded simultaneously from the aortic isthmus and ductus arteriosus of a 20-weeks fetus using a large sample volume demonstrating that blood flow in the aortic isthmus starts and peaks earlier than in the ductus arteriosus. Note the brief late systolic reversal of blood flow in the aortic isthmus. *Figure by the courtesy of G. Acharya.*

Vessel diameter is an important factor for the volume blood flow calculations and an error can cause significant differences in results. We used modern ultrasound equipment with high-resolution capability, performed measurements on zoomed images and used an average of three measurements to improve measurement precision (Kiserud & Rasmussen, 1998; Kiserud et al, 1999). The velocity profile of the aorta, pulmonary artery and the aortic isthmus was assumed to be flat, i.e. a spatial velocity profile coefficient of 1.0 while calculating the volume blood flow.

Methods other than B-mode ultrasonography, such as M-mode ultrasound, power Doppler angiography, B-flow, may be used for measuring vessel diameter. However, their accuracy has not been validated. Recently, fetal CO measurements using newer technologies such as four-dimensional echocardiography with STIC (spatio-temporal image correlation) and VOCAL (virtual organ computer-aided analysis) (Rizzo et al, 2007; Messing et al, 2007; Molina et al, 2008) have been shown to be feasible, but their accuracy remains to be further investigated.

Safety issues

We strictly adhered to the ALARA principle while performing ultrasonography. In study I, fetuses were exposed to B-mode ultrasonography only. A vaginal transducer was used, and an I_{spta} of 720 mW/cm² was the upper output limit of the ultrasound machine. The data collection was performed in a setting of routine first trimester screening for chromosome defects using nuchal translucency measurement and the entire session lasted a maximum of 20 minutes.

In study II and III, the examination sessions lasted approximately 30 minutes. A vaginal transducer with a central frequency of about 7.5 MHz was used during the first examination at 11 – 14 weeks. An abdominal probe with a central frequency of approximately, 3.5 MHz was used during the subsequent visits. An I_{spta} of 720 mW/cm² was the upper output limit of the ultrasound machine. We used colour Doppler to identify the direction of blood flow, but it was applied for a few seconds at time. Pulsed-wave Doppler was used for very short periods to obtain representative blood flow velocity waveforms only from the desired blood vessels and the fetal head was not exposed to Doppler at any time.

Validity

It is important to establish the reliability of a measurement technique and show that it measures something in a consistent manner. Furthermore, for a measurement to be clinically useful, its validity has to be confirmed by demonstrating that it measures what is intended to measure. The accuracy of fetal cardiac output (Shiraishi et al, 1993) and placental volume blood flow measurements using ultrasonography have been validated in animal (Schmidt et al, 1991; Sokol et al, 1996; Barbera et al, 1999) and in vitro (Rasmussen, 1987) experiments. Reproducibility of cardiac output (Räsänen et al, 1996) and Q_{uv} measurements (Figueras et al, 2008) in human fetuses has been shown to be reasonably good. Results of intra-observer reproducibility of volume blood flow measurements in our studies were within the acceptable range.

The reference intervals were constructed using data obtained from an unselected but homogenous Finnish population. Therefore, it could be argued that our results may not be valid outside the Nordic population and the external validity may be questioned. However, the ethnicity is unlikely to be an important factor as volume blood flows were normalized by the fetal weight.

CONCLUSIONS

Fetal heart structures can be examined reliably in a majority of cases in the late first trimester using transvaginal ultrasonography. We have established cross-sectional references ranges for the evaluation of some cardiac structures at 11-14 weeks of gestation. Furthermore, we have established references ranges for the serial measurement of Q_{uv}, Q_{ai} and cardiac ventricular outputs at 11-20 weeks of gestation. Placental volume blood flow and the fraction of CCO distributed to the placenta increases substantially during 11-20 weeks of gestation reflecting faster placental growth relative to fetal growth and establishment of a low resistance placental circulation during the first half of pregnancy. The fraction of cardiac output directed to the upper body and brain is relatively small but fairly constant during 11-20 weeks of gestation.

FUTURE ASPECTS

Significant advances have been made in the last two decades in the field of fetal cardiology with steadily improving detection rates for congenital heart defects. The main focus in recent years has been early screening and detection of structural anomalies, but not so much emphasis has been put on the physiological aspects. Even the gestational age related physiological changes in fetal cardiovascular system are not well defined yet. Experimental animal studies using invasive methods are useful in validating ultrasound techniques (Acharya et al, 2004; Acharya et al, 2007; Acharya et al, 2008; Kiserud et al, 1999; Schmidt et al, 1990; Schmidt et al, 1991; Shiraisi et al, 1993). However, inter-species differences restrict direct application of physiological data obtained from animal fetuses to humans. Despite limitations, non-invasive volume blood flow measurements may provide better insight into human fetal circulatory physiology. It could be desirable to use this simple non-invasive method together with other commonly used qualitative and semi-quantitative Doppler indices in the assessment of fetal wellbeing and management of high-risk pregnancies. Whether such an approach would help improving perinatal and long-term outcomes, merits further investigation.

REFERENCES

1. Abramowicz JS, Barnett SB, Duck FA, Edmonds PD, Hynynen KH, Ziskin MC (2008) Fetal thermal effects of diagnostic ultrasound. *J Ultrasound Med* **27**: 541-59
2. Acharya G (2009) Technical aspects of aortic isthmus Doppler velocimetry in human fetuses. *Ultrasound Obstet Gynecol* **33**: 628-633
3. Acharya G, Erkinaro T, Mäkikallio K, Lappalainen T, Rasanen J (2004). Relationships among Doppler-derived umbilical artery absolute velocities, cardiac function, and placental volume blood flow and resistance in fetal sheep. *Am J Physiol Heart Circ Physiol* **286**: H1266-72
4. Acharya G, Räsänen J, Kiserud T, Huhta JC (2006) The fetal cardiac function. *Current Cardiology Reviews* **2**: 41-53
5. Acharya G, Räsänen J, Mäkikallio K, Erkinaro T, Kavasmaa T, Haapsamo M, Mertens L, Huhta JC (2008) Metabolic acidosis decreases fetal myocardial isovolumic velocities in a chronic sheep model of increased placental vascular resistance. *Am J Physiol Heart Circ Physiol* **294**: H498-504
6. Acharya G and Sitras V (2009) Oxygen uptake of the human fetus at term. *Acta Obstet Gynecol Scand* **88**: 104-109
7. Acharya G, Sitras V, Erkinaro T, Mäkikallio K, Kavasmaa T, Päkkilä M, Huhta JC, Räsänen J (2007) Experimental validation of uterine artery volume blood flow measurement by Doppler ultrasonography in pregnant sheep. *Ultrasound Obstet Gynecol* **29**: 401-406
8. Acharya G, Wilsgaard T, Rosvold Berntsen GK, Maltau JM, Kiserud T (2005a) Reference ranges for umbilical vein blood flow in the second half of pregnancy based on longitudinal data. *Prenat Diagn* **25**: 99-111
9. Acharya G, Wilsgaard T, Berntsen GK, Maltau JM, Kiserud T (2005b). Reference ranges for serial measurements of umbilical artery Doppler indices in the second half of pregnancy. *Am J Obstet Gynecol* **192** :937-944
10. Acharya G, Wilsgaard T, Berntsen GK, Maltau JM, Kiserud T (2005c). Reference ranges for serial measurements of blood velocity and pulsatility index at the intra-abdominal portion, and fetal and placental ends of the umbilical artery. Ultrasound Obstet Gynecol **26**: 162-169

11. Alfirevic Z and Neilson JP (1995) Doppler ultrasonography in high-risk pregnancies: systematic review with meta-analysis. *Am J Obstet Gynecol* **172**: 1379-1387
12. Allan L (2006) Screening the fetal heart. *Ultrasound Obstet Gynecol* **28**: 5-7
13. Allan LD (2003) Cardiac anatomy screening: what is the best time for screening in pregnancy? *Curr Opin Obstet Gynecol* **15**: 143-146
14. Almstrom H and Sonesson SE (1996) Doppler echocardiographic assessment of fetal blood flow redistribution during maternal hyperoxygenation. *Ultrasound Obstet Gynecol* **8**: 256-261
15. Anderson PA, Glick KL, Killam AP, Mainwaring RD (1986) The effect of heart rate on in utero left ventricular output in the fetal sheep. *J Physiol* **372**: 557-573
16. Anderson PA, Killam AP, Mainwaring RD, Oakeley AE (1987) In utero right ventricular output in the fetal lamb: the effect of heart rate. *J Physiol* **387**: 297-316
17. Assali NS, Rauramo L, Peltonen T (1960) Measurement of uterine blood flow and uterine metabolism. VIII. Uterine and fetal blood flow and oxygen consumption in early human pregnancy. *Am J Obstet Gynecol* **79**: 86-98
18. Assali NS, Douglas RA,Jr, Baird WW, Nicholson DB, Suyemoto R (1953) Measurement of uterine blood flow and uterine metabolism. IV. Results in normal pregnancy. *Am J Obstet Gynecol* **66**: 248-253
19. Ball RH and Parer JT (1992) The physiologic mechanisms of variable decelerations. *Am J Obstet Gynecol* **166**: 1683-1688
20. Barbera A, Galan HL, Ferrazzi E, Rigano S, Jozwik M, Battaglia FC, Pardi G (1999) Relationship of umbilical vein blood flow to growth parameters in the human fetus. *Am J Obstet Gynecol* **181**: 174-179
21. Barcroft J (1946) Researches on pre-natal life. Blackwell Scientific Publications: Oxford
22. Barnett SB (2000) Biophysical aspects of diagnostic ultrasound. *Ultrasound Med Biol* **26 Suppl 1**: S68-70
23. Barnett SB, Maulik D, International Perinatal Doppler Society (2001) Guidelines and recommendations for safe use of Doppler ultrasound in perinatal applications. *J Matern Fetal Med* **10**: 75-84
24. Bartlett JW and Frost C (2008) Reliability, repeatability and reproducibility: analysis of measurement errors in continuous variables. *Ultrasound Obstet Gynecol* **31**: 466-475
25. Bellotti M, Pennati G, De Gasperi C, Battaglia FC, Ferrazzi E (2000) Role of ductus venosus in distribution of umbilical blood flow in human fetuses during second half of pregnancy. *Am J Physiol Heart Circ Physiol* **279**: H1256-263

26. Bers DM (2002) Cardiac excitation-contraction coupling. *Nature* **415**: 198-205
27. Blaas HG and Eik-Nes SH (2009) Sonoembryology and early prenatal diagnosis of neural anomalies. *Prenat Diagn **29**:*312-25
28. Bonds DR, Crosby LO, Cheek TG, Hagerdal M, Gutsche BB, Gabbe SG (1986) Estimation of human fetal-placental unit metabolic rate by application of the Bohr principle. *J Dev Physiol* **8**: 49-54
29. Brace RA (1983) Fetal blood volume responses to acute fetal hemorrhage. *Circ Res* **52**: 730-734
30. Braunwald E (1977) Determinants and assessment of cardiac function. *N Engl J Med* **296**: 86-89
31. Braunwald E (1971) Control of myocardial oxygen consumption: physiologic and clinical considerations. *Am J Cardiol* **27**: 416-432
32. Bruneau BG (2008) The developmental genetics of congenital heart disease. *Nature* **451**: 943-948
33. Carceller-Blanchard AM and Fouron JC (1993) Determinants of the Doppler flow velocity profile through the mitral valve of the human fetus. *Br Heart J* **70**: 457-460
34. Carvalho JS, Ho SY, Shinebourne EA (2005) Sequential segmental analysis in complex fetal cardiac abnormalities: a logical approach to diagnosis. *Ultrasound Obstet Gynecol* **26**: 105-111
35. Castle B and Mackenzie IZ (1986). In vivo observations on intravascular blood pressure in the fetus during mid-pregnancy. *Fetal Physiological Measurements*. Edited by P. Rolfe,. London, Butterworths. pp. 65-69
36. Clur SA, Mathijssen IB, Pajkrt E, Cook A, Laurini RN, Ottenkamp J, Bilardo CM (2008) Structural heart defects associated with an increased nuchal translucency: 9 years experience in a referral centre. *Prenat Diagn* **28**: 347-354
37. Clyman RI, Mauray F, Roman C, Rudolph AM (1978) PGE2 is a more potent vasodilator of the lamb ductus arteriosus than is either PGI2 or 6 keto PGF1alpha. *Prostaglandins* **16**: 259-264
38. Coceani F and Olley PM (1988) The control of cardiovascular shunts in the fetal and perinatal period. *Can J Physiol Pharmacol* **66**: 1129-1134
39. Cook AC (2001) The spectrum of fetal cardiac malformations. *Cardiol Young* **11**: 97-110
40. Cook AC, Yates RW, Anderson RH (2004) Normal and abnormal fetal cardiac anatomy. *Prenat Diagn* **24**: 1032-1048

41. Dehmer GJ, Firth BG, Hillis LD (1982) Oxygen consumption in adult patients during cardiac catheterization. *Clin Cardiol* **5**: 436-40.
42. Dekaban AS (1978) Changes in brain weights during the span of human life: relation of brain weights to body heights and body weights. *Ann Neurol* **4**: 345-356
43. de Paula CF, Ruano R, Campos JA, Zugaib M (2008) Placental volumes measured by 3-dimensional ultrasonography in normal pregnancies from 12 to 40 weeks' gestation. *J Ultrasound Med* **27**: 1583-1590
44. Del Rio M, Martinez JM, Figueras F, Bennasar M, Olivella A, Palacio M, Coll O, Puerto B, Gratacos E (2008) Doppler assessment of the aortic isthmus and perinatal outcome in preterm fetuses with severe intrauterine growth restriction. *Ultrasound Obstet Gynecol* **31**: 41-47
45. DeVore GR, Siassi B, Platt LD (1984) Fetal echocardiography. IV. M-mode assessment of ventricular size and contractility during the second and third trimesters of pregnancy in the normal fetus. *Am J Obstet Gynecol* **150**: 981-988
46. Divon MY, Zimmer EZ, Platt LD, Paldi E (1985) Human fetal breathing: associated changes in heart rate and beat-to-beat variability. *Am J Obstet Gynecol* **151**: 403-406
47. Dolkart LA and Reimers FT (1991) Transvaginal fetal echocardiography in early pregnancy: normative data. *Am J Obstet Gynecol* **165**: 688-691
48. Falcon O, Faiola S, Huggon I, Allan L, Nicolaides KH (2006) Fetal tricuspid regurgitation at the 11 + 0 to 13 + 6-week scan: association with chromosomal defects and reproducibility of the method. *Ultrasound Obstet Gynecol* **27**: 609-612
49. Ferrazzi E, Bozzo M, Rigano S, Bellotti M, Morabito A, Pardi G, Battaglia FC, Galan HL (2002) Temporal sequence of abnormal Doppler changes in the peripheral and central circulatory systems of the severely growth-restricted fetus. *Ultrasound Obstet Gynecol* **19**: 140-146
50. Figueras F, Benavides A, Del Rio M, Crispi F, Eixarch E, Martinez JM, Hernandez-Andrade E, Gratacós E (2009). Monitoring of fetuses with intrauterine growth restriction: longitudinal changes in ductus venosus and aortic isthmus flow. *Ultrasound Obstet Gynecol* 33: 39-43.
51. Figueras F, Fernandez S, Hernandez-Andrade E, Gratacos E (2008) Umbilical venous blood flow measurement: accuracy and reproducibility. *Ultrasound Obstet Gynecol* **32**: 587-591
52. Fouron JC (2003) The unrecognized physiological and clinical significance of the fetal aortic isthmus. *Ultrasound Obstet Gynecol* **22**: 441-447

53. Fouron JC, Skoll A, Sonesson SE, Pfizenmaier M, Jaeggi E, Lessard M (1999). Relationship between flow through the fetal aortic isthmus and cerebral oxygenation during acute placental circulatory insufficiency in ovine fetuses. *Am J Obstet Gynecol* **181**: 1102-1107.
54. Friedman WF (1972) The intrinsic physiologic properties of the developing heart. *Prog Cardiovasc Dis* **15**: 87-111
55. Gembruch U, Knopfle G, Bald R, Hansmann M (1993) Early diagnosis of fetal congenital heart disease by transvaginal echocardiography. *Ultrasound Obstet Gynecol* **3**: 310-317
56. Gembruch U, Shi C, Smrcek JM (2000) Biometry of the fetal heart between 10 and 17 weeks of gestation. *Fetal Diagn Ther* **15**: 20-31
57. Gilbert-Barness and Debich-Spicer (2004) Abnormalities of the placenta. In *Embryo & Fetal Pathology. Colour Atlas with Ultrasound Correlation*. Edited by E. Gilbert-Barness and D. Debich-Spicer, Cambridge University Press. Pp. 150-79
58. Giles WB, Trudinger BJ, Baird PJ (1985) Fetal umbilical artery flow velocity waveforms and placental resistance: pathological correlation. *Br J Obstet Gynaecol* **92**: 31-38
59. Grannum PA, Berkowitz RL, Hobbins JC (1979) The ultrasonic changes in the maturing placenta and their relation to fetal pulmonic maturity. *Am J Obstet Gynecol* **133**: 915-922
60. Grant DA (1999) Ventricular constraint in the fetus and newborn. *Can J Cardiol* **15**: 95-104
61. Haak MC, Bartelings MM, Gittenberger-De Groot AC, Van Vugt JM (2002) Cardiac malformations in first-trimester fetuses with increased nuchal translucency: ultrasound diagnosis and postmortem morphology. *Ultrasound Obstet Gynecol* **20**: 14-21
62. Harper AM (1965) Physiology of Cerebral Bloodflow. *Br J Anaesth* **37**: 225-235
63. Haugen G, Kiserud T, Godfrey K, Crozier S, Hanson M (2004) Portal and umbilical venous blood supply to the liver in the human fetus near term. *Ultrasound Obstet Gynecol* **24**: 599-605
64. Hernandez-Andrade E, Figueroa-Diesel H, Kottman C, Illanes S, Arraztoa J, Acosta-Rojas R, Gratacos E (2007) Gestational-age-adjusted reference values for the modified myocardial performance index for evaluation of fetal left cardiac function. *Ultrasound Obstet Gynecol* **29**: 321-325
65. Hill LM, Guzick D, Fries J, Hixson J, Rivello D (1990) The transverse cerebellar diameter in estimating gestational age in the large for gestational age fetus. *Obstet Gynecol* **75**: 981-985

66. Hofstaetter C, Hansmann M, Eik-Nes SH, Huhta JC, Luther SL (2006) A cardiovascular profile score in the surveillance of fetal hydrops. *J Matern Fetal Neonatal Med* **19**: 407-413
67. Huggon IC, Turan O, Allan LD (2004) Doppler assessment of cardiac function at 11-14 weeks' gestation in fetuses with normal and increased nuchal translucency. *Ultrasound Obstet Gynecol* **24**: 390-398
68. Huhta JC (2005) Fetal congestive heart failure. *Semin Fetal Neonatal Med* **10**: 542-552
69. Huhta JC (2004) Guidelines for the evaluation of heart failure in the fetus with or without hydrops. *Pediatr Cardiol* **25**: 274-286
70. Huhta JC, Cohen M, Gutgesell HP (1984) Patency of the ductus arteriosus in normal neonates: two-dimensional echocardiography versus Doppler assessment. *J Am Coll Cardiol* **4**: 561-564
71. Hyett JA, Perdu M, Sharland GK, Snijders RS, Nicolaides KH (1997) Increased nuchal translucency at 10-14 weeks of gestation as a marker for major cardiac defects. *Ultrasound Obstet Gynecol* **10**: 242-246
72. Jackson MR, Mayhew TM, Boyd PA (1992) Quantitative description of the elaboration and maturation of villi from 10 weeks of gestation to term. *Placenta* **13**: 357-370
73. Jensen A, Garnier Y, Berger R (1999) Dynamics of fetal circulatory responses to hypoxia and asphyxia. *Eur J Obstet Gynecol Reprod Biol* **84**: 155-172
74. Jensen A, Roman C, Rudolph AM (1991) Effects of reducing uterine blood flow on fetal blood flow distribution and oxygen delivery. *J Dev Physiol* **15**: 309-323
75. Johnson P, Maxwell DJ, Tynan MJ, Allan LD (2000) Intracardiac pressures in the human fetus. *Heart* **84**: 59-63
76. Johnson P, Sharland G, Maxwell D, Allan L (1992) The role of transvaginal sonography in the early detection of congenital heart disease. *Ultrasound Obstet Gynecol* **2**: 248-251
77. Jou HJ, Shyu MK, Wu SC, Chen SM, Su CH, Hsieh FJ (1998) Ultrasound measurement of the fetal cavum septi pellucidi. *Ultrasound Obstet Gynecol* **12**: 419-421
78. Kanzaki T and Chiba Y (1990) Evaluation of the preload condition of the fetus by inferior vena caval blood flow pattern. *Fetal Diagn Ther* **5**: 168-174
79. Kenny JF, Plappert T, Doubilet P, Saltzman DH, Cartier M, Zollars L, Leatherman GF, St John Sutton MG (1986) Changes in intracardiac blood flow velocities and right and left ventricular stroke volumes with gestational age in the normal human fetus: a prospective Doppler echocardiographic study. *Circulation* **74**: 1208-1216

80. Kessler J, Rasmussen S, Godfrey K, Hanson M, Kiserud T (2008) Longitudinal study of umbilical and portal venous blood flow to the fetal liver: low pregnancy weight gain is associated with preferential supply to the fetal left liver lobe. *Pediatr Res* **63**: 315-320
81. Kessler J, Rasmussen S, Kiserud T (2007a) The fetal portal vein: normal blood flow development during the second half of human pregnancy. *Ultrasound Obstet Gynecol* **30**: 52-60
82. Kessler J, Rasmussen S, Kiserud T (2007b) The left portal vein as an indicator of watershed in the fetal circulation: development during the second half of pregnancy and a suggested method of evaluation. *Ultrasound Obstet Gynecol* **30**: 757-764
83. Kety SS (1950) Circulation and metabolism of the human brain in health and disease. *Am J Med* **8**: 205-217
84. Kilavuz O, Vetter K, Kiserud T, Vetter P (2003) The left portal vein is the watershed of the fetal venous system. *J Perinat Med* **31**: 184-187,
85. Kiserud T (2005) Physiology of the fetal circulation. *Semin Fetal Neonatal Med* **10**: 493-503
86. Kiserud T and Acharya G (2004) The fetal circulation. *Prenat Diagn* **24**: 1049-1059
87. Kiserud T, Ebbing C, Kessler J, Rasmussen S (2006) Fetal cardiac output, distribution to the placenta and impact of placental compromise. *Ultrasound Obstet Gynecol* **28**: 126-136
88. Kiserud T, Hellevik LR, Eik-Nes SH, Angelsen BA, Blaas HG (1994) Estimation of the pressure gradient across the fetal ductus venosus based on Doppler velocimetry. *Ultrasound Med Biol* **20**: 225-232
89. Kiserud T, Kilavuz O, Hellevik LR (2003) Venous pulsation in the fetal left portal branch: the effect of pulse and flow direction. *Ultrasound Obstet Gynecol* **21**: 359-364
90. Kiserud T and Rasmussen S (2001) Ultrasound assessment of the fetal foramen ovale. *Ultrasound Obstet Gynecol* **17**: 119-124
91. Kiserud T and Rasmussen S (1998) How repeat measurements affect the mean diameter of the umbilical vein and the ductus venosus. *Ultrasound Obstet Gynecol* **11**: 419-425
92. Kiserud T, Rasmussen S, Skulstad S (2000) Blood flow and the degree of shunting through the ductus venosus in the human fetus. *Am J Obstet Gynecol* **182**: 147-153
93. Kiserud T, Saito T, Ozaki T, Rasmussen S, Hanson MA (1999) Validation of diameter measurements by ultrasound: intraobserver and interobserver variations assessed in vitro and in fetal sheep. *Ultrasound Obstet Gynecol* **13**: 52-57

94. Konje JC, Taylor DJ, Rennie MJ (1996) Application of ultrasonic transit time flowmetry to the measurement of umbilical vein blood flow at caesarean section. *Br J Obstet Gynaecol* **103**: 1004-1008

95. Lee W, Allan L, Carvalho JS, Chaoui R, Copel J, Devore G, Hecher K, Munoz H, Nelson T, Paladini D, Yagel S, ISUOG Fetal Echocardiography Task Force (2008) ISUOG consensus statement: what constitutes a fetal echocardiogram? *Ultrasound Obstet Gynecol* **32**: 239-242

96. Lewis AB, Heymann MA, Rudolph AM (1976) Gestational changes in pulmonary vascular responses in fetal lambs in utero. *Circ Res* **39**: 536-541

97. Lucas W, Kirschbaum T, Assali NS (1966) Cephalic circulation and oxygen consumption before and after birth. *Am J Physiol* **210**: 287-292

98. Mahony BS, Callen PW, Filly RA, Hoddick WK (1984) The fetal cisterna magna. *Radiology* **153**: 773-776

99. Mahony L and Jones LR (1986) Developmental changes in cardiac sarcoplasmic reticulum in sheep. *J Biol Chem* **261**: 15257-15265

100. Mäkikallio K, Erkinaro T, Niemi N, Kavasmaa T, Acharya G, Päkkilä M, Räsänen J (2006). Fetal oxygenation and Doppler ultrasonography of cardiovascular hemodynamics in a chronic near-term sheep model. *Am J Obstet Gynecol* 194: 542-550

101. Mäkikallio K, Räsänen J, Mäkikallio T, Vuolteenaho O, Huhta JC (2008) Human fetal cardiovascular profile score and neonatal outcome in intrauterine growth restriction. *Ultrasound Obstet Gynecol* **31**: 48-54

102. Mäkikallio K, Tekay A, Jouppila P (2004) Uteroplacental hemodynamics during early human pregnancy: a longitudinal study. *Gynecol Obstet Invest* **58**: 49-54

103. Makrydimas G, Sotiriadis A, Ioannidis JP (2003) Screening performance of first-trimester nuchal translucency for major cardiac defects: a meta-analysis. *Am J Obstet Gynecol* **189**: 1330-1335

104. Malas MA, Sulak O, Gökçimen A, Sari A (2003) Morphology of umbilical vessels in human fetuses: a quantitative light microscope study. *Eur J Morphol* **41**: 167-74

105. McAuliffe FM, Hornberger LK, Winsor S, Chitayat D, Chong K, Johnson JA (2004) Fetal cardiac defects and increased nuchal translucency thickness: a prospective study. *Am J Obstet Gynecol* **191**: 1486-1490

106. Messing B, Cohen SM, Valsky DV, Rosenak D, Hochner-Celnikier D, Savchev S, Yagel S (2007) Fetal cardiac ventricle volumetry in the second half of gestation assessed by 4D ultrasound using STIC combined with inversion mode. *Ultrasound Obstet Gynecol* **30**: 142-151

107. Metcalfe J, Romney SL, Ramsey LH, Reid DE, Burwell CS (1955) Estimation of uterine blood flow in normal human pregnancy at term. *J Clin Invest* **34**: 1632-1638

108. Mielke G and Benda N (2001) Cardiac output and central distribution of blood flow in the human fetus. *Circulation* **103**: 1662-1668

109. Molina FS, Faro C, Sotiriadis A, Dagklis T, Nicolaides KH (2008). Heart stroke volume and cardiac output by four-dimensional ultrasound in normal fetuses. *Ultrasound Obstet Gynecol* 32:181-187

110. Molteni RA (1984) Placental growth and fetal/placental weight (F/P) ratios throughout gestation--their relationship to patterns of fetal growth. *Semin Perinatol* **8**: 94-100

111. Molteni RA, Stys SJ, Battaglia FC (1978) Relationship of fetal and placental weight in human beings: fetal/placental weight ratios at various gestational ages and birth weight distributions. *J Reprod Med* **21**: 327-334

112. Monteagudo A and Timor-Tritsch IE (2008) Normal sonographic development of the central nervous system from the second trimester onwards using 2D, 3D and transvaginal sonography. *Prenat Diagn **29**:326-39*

113. Moorman A, Webb S, Brown NA, Lamers W, Anderson RH (2003) Development of the heart: (1) formation of the cardiac chambers and arterial trunks. *Heart* **89**: 806-814

114. Morris JA, Hustead RF, Robinson RG, Haswell GL (1974) Measurement of fetoplacental blood volume in the human previable fetus. *Am J Obstet Gynecol* **118**: 927-934

115. Muller F and O'Rahilly R (2006) The amygdaloid complex and the medial and lateral ventricular eminences in staged human embryos. *J Anat* **208**: 547-564

116. Naeye RL (1985) Umbilical cord length: clinical significance. *J Pediatr* **107**: 278-281

117. Nicolaides KH, Economides DL, Soothill PW (1989) Blood gases, pH, and lactate in appropriate- and small-for-gestational-age fetuses. *Am J Obstet Gynecol* **161**: 996-1001

118. O'Rahilly R and Muller F (2008) Significant features in the early prenatal development of the human brain. *Ann Anat* **190**: 105-118

119. O'Rahilly R and Muller F (2007) The development of the neural crest in the human. *J Anat* **211**: 335-351

120. Patton DJ and Fouron JC (1995) Cerebral arteriovenous malformation: prenatal and postnatal central blood flow dynamics. *Pediatr Cardiol* **16**: 141-144
121. Pearce, W. (2006) Hypoxic regulation of the fetal cerebral circulation. *Journal of Applied Physiology* **100**: 731-738
122. Pennati G, Bellotti M, De Gasperi C, Rognoni G (2004) Spatial velocity profile changes along the cord in normal human fetuses: can these affect Doppler measurements of venous umbilical blood flow? *Ultrasound Obstet Gynecol* **23**: 131-137
123. Phillipos EZ, Robertson MA, Still KD (1994) The echocardiographic assessment of the human fetal foramen ovale. *J Am Soc Echocardiogr* **7**: 257-263
124. Pilu G, Reece EA, Goldstein I, Hobbins JC, Bovicelli L (1989) Sonographic evaluation of the normal developmental anatomy of the fetal cerebral ventricles: II. The atria. *Obstet Gynecol* **73**: 250-256
125. Poston L (1997) The control of blood flow to the placenta. *Exp Physiol* **82**: 377-387
126. Räsänen J, Debbs RH, Wood DC, Weiner S, Weil SR, Huhta JC (1997) Human fetal right ventricular ejection force under abnormal loading conditions during the second half of pregnancy. *Ultrasound Obstet Gynecol* **10**: 325-332
127. Räsänen J, Kirkinen P, Jouppila P (1989) Right ventricular dysfunction in human fetal compromise. *Am J Obstet Gynecol* **161**: 136-140
128. Räsänen J, Wood DC, Debbs RH, Cohen J, Weiner S, Huhta JC (1998) Reactivity of the human fetal pulmonary circulation to maternal hyperoxygenation increases during the second half of pregnancy: a randomized study. *Circulation* **97**: 257-262
129. Räsänen J, Wood DC, Weiner S, Ludomirski A, Huhta JC (1996) Role of the pulmonary circulation in the distribution of human fetal cardiac output during the second half of pregnancy. *Circulation* **94**: 1068-1073
130. Rasmussen K (1987) Precision and accuracy of Doppler flow measurements. In vitro and in vivo study of the applicability of the method in human fetuses. *Scand J Clin Lab Invest* **47**: 311-318
131. Reller MD, McDonald RW, Gerlis LM, Thornburg KL (1991) Cardiac embryology: basic review and clinical correlations. *J Am Soc Echocardiogr* **4**: 519-532
132. Respondek M, Respondek A, Huhta JC, Wilczynski J (1992) 2D echocardiographic assessment of the fetal heart size in the 2nd and 3rd trimester of uncomplicated pregnancy. *Eur J Obstet Gynecol Reprod Biol* **44**: 185-188

133. Respondek ML, Kammermeier M, Ludomirsky A, Weil SR, Huhta JC (1994) The prevalence and clinical significance of fetal tricuspid valve regurgitation with normal heart anatomy. *Am J Obstet Gynecol* **171**: 1265-1270

134. Rizzo G, Capponi A, Cavicchioni O, Vendola M, Arduini D (2007) Fetal cardiac stroke volume determination by four-dimensional ultrasound with spatio-temporal image correlation compared with two-dimensional and Doppler ultrasonography. *Prenat Diagn* **27**: 1147-1150

135. Rizzo G, Capponi A, Rinaldo D, Arduini D, Romanini C (1995) Ventricular ejection force in growth-retarded fetuses. *Ultrasound Obstet Gynecol* **5**: 247-255

136. Rizzo G, Capponi A, Vendola M, Pietrolucci ME, Arduini D (2008) Relationship between aortic isthmus and ductus venosus velocity waveforms in severe growth restricted fetuses. *Prenat Diagn* **28**: 1042-1047

137. Royston P (1995) Calculation of unconditional and conditional reference intervals for foetal size and growth from longitudinal measurements. *Stat Med* **14**: 1417-1436

138. Royston P and Altman DG (1995) Design and analysis of longitudinal studies of fetal size. *Ultrasound Obstet Gynecol* **6**: 307-312

139. Royston P and Wright EM (1998) How to construct 'normal ranges' for fetal variables. *Ultrasound Obstet Gynecol* **11**: 30-38

140. Rudolph AM, Heymann MA, Teramo K, Barrett C, Räihä N (1971) Studies on the circulation of the previable human fetus. *Pediatr Res* **5**: 452-465

141. Rudolph AM (2009) The fetal circulation. In Congenital diseases of the Heart: Clinical-Pathological Considerations. 3rd edition. Wiley-Blackwell. Chapter 1. Pp. 1-24

142. Rudolph AM (1985) Distribution and regulation of blood flow in the fetal and neonatal lamb. *Circ Res* **57**: 811-821

143. Rumack CM, Wilson SR, Charbonneau JW (2008) Diagnostic Ultrasound, 3rd edition. Mosby

144. Salvesen KA and Eik-Nes SH (1999) Ultrasound during pregnancy and subsequent childhood non-right handedness: a meta-analysis. *Ultrasound Obstet Gynecol* **13**: 241-246

145. Salvesen KA and Lees C (2009) Ultrasound is not unsound, but safety is an issue. *Ultrasound Obstet Gynecol* **33**: 502-505

146. Sand AE, Andersson E, Fried G (2002) Effects of nitric oxide donors and inhibitors of nitric oxide signalling on endothelin- and serotonin-induced contractions in human placental arteries. *Acta Physiol Scand* **174**: 217-223

147. Sariola H, Frilander M, Heino T, Jernvall J, Partanen J, Sainio K, Salminen M, Thesleff I (eds) (2003) Kehitysbiologia, solusta yksilöksi. Duodecim
148. Schmidt KG, Di Tommaso M, Silverman NH, Rudolph AM (1991) Doppler echocardiographic assessment of fetal descending aortic and umbilical blood flows. Validation studies in fetal lambs. *Circulation* **83**: 1731-1737
149. Schmidt KG, Silverman NH, van Hare GF, Hawkins JA, Cloez, JL, Rudolph AM (1990) Two-dimensional echocardiographic determination of ventricular volumes in the fetal heart. Validation studies in fetal lambs. *Circulation* **81**: 325-333
150. Schmidt U, Hajjar RJ, Gwathmey JK (1995) The force-interval relationship in human myocardium. *J Card Fail* **1**: 311-321
151. Sedmera D and McQuinn T (2008) Embryogenesis of the heart muscle. *Heart Fail Clin* **4**: 235-245
152. Severi FM, Rizzo G, Bocchi C, D'Antona D, Verzuri MS, Arduini D (2000) Intrauterine growth retardation and fetal cardiac function. *Fetal Diagn Ther* **15**: 8-19
153. Shiraishi H, Silverman NH, Rudolph AM (1993) Accuracy of right ventricular output estimated by Doppler echocardiography in the sheep fetus. *Am J Obstet Gynecol* **168**: 947-953
154. Silverman NH and Schmidt KG (1990) Ventricular volume overload in the human fetus: observations from fetal echocardiography. *J Am Soc Echocardiogr* **3**: 20-29
155. Sokol GM, Liechty EA, Boyle DW (1996) Comparison of steady-state diffusion and transit time ultrasonic measurements of umbilical blood flow in the chronic fetal sheep preparation. *Am J Obstet Gynecol* **174**: 1456-1460
156. Sonesson SE and Fouron JC (1997) Doppler velocimetry of the aortic isthmus in human fetuses with abnormal velocity waveforms in the umbilical artery. *Ultrasound Obstet Gynecol* **10**: 107-111
157. Soothill PW, Nicolaides KH, Rodeck CH, Gamsu H (1986) Blood gases and acid-base status of the human second-trimester fetus. *Obstet Gynecol* **68**: 173-176
158. Struijk PC, Mathews VJ, Loupas T, Stewart PA, Clark EB, Steegers EA, Wladimiroff JW (2008) Blood pressure estimation in the human fetal descending aorta. *Ultrasound Obstet Gynecol* **32**: 673-681
159. Sutton MS, Gill T, Plappert T, Saltzman DH, Doubilet P (1991) Assessment of right and left ventricular function in terms of force development with gestational age in the normal human fetus. *Br Heart J* **66**: 285-289

160. Sutton MS, Theard MA, Bhatia SJ, Plappert T, Saltzman DH, Doubilet P (1990) Changes in placental blood flow in the normal human fetus with gestational age. *Pediatr Res* **28**: 383-387

161. Tanaka H, Senoh D, Yanagihara T, Hata T (2000) Intrauterine sonographic measurement of embryonic brain vesicle. *Hum Reprod* **15**: 1407-1412

162. Tanimura T, Nelson T, Hollingsworth RR, Shepard TH (1971) Weight standards for organs from early human fetuses. *Anat Rec* **171**: 227-236

163. Tegnander E and Eik-Nes SH (2006) The examiner's ultrasound experience has a significant impact on the detection rate of congenital heart defects at the second-trimester fetal examination. *Ultrasound Obstet Gynecol* **28**: 8-14

164. Tongsong T and Boonyanurak P (2004) Placental thickness in the first half of pregnancy. *J Clin Ultrasound* **32**: 231-234

165. Tulzer G, Gudmundsson S, Rotondo KM, Wood DC, Yoon GY, Huhta JC (1991a) Acute fetal ductal occlusion in lambs. *Am J Obstet Gynecol* **165**: 775-778

166. Tulzer G, Gudmundsson S, Rotondo KM, Wood DC, Cohen AW, Huhta JC (1991b). Doppler in the evaluation and prognosis of fetuses with tricuspid regurgitation. J Matern Fetal Invest. 19991;1:15-18. tricuspid regurgitation. *J Matern Fetal Invest* **1**:15-18

167. Tulzer G, Khowsathit P, Gudmundsson S, Wood DC, Tian ZY, Schmitt K, Huhta JC (1994) Diastolic function of the fetal heart during second and third trimester: a prospective longitudinal Doppler-echocardiographic study. *Eur J Pediatr* **153**: 151-154

168. Ursem NT, Struijk PC, Hop WC, Clark EB, Keller BB, Wladimiroff JW (1998) Heart rate and flow velocity variability as determined from umbilical Doppler velocimetry at 10-20 weeks of gestation. *Clin Sci (Lond)* **95**: 539-545

169. Walsh SZ, Meyer WW, Lind J (1974). The human fetal and neonatal circulation: Function and structure. Charles C Thomas Publishers, Springfield, Illinois, USA.

170. van der Mooren K, Barendregt LG, Wladimiroff JW (1991) Fetal atrioventricular and outflow tract flow velocity waveforms during normal second half of pregnancy. *Am J Obstet Gynecol* **165**: 668-674

171. van Splunder IP and Wladimiroff JW (1996) Cardiac functional changes in the human fetus in the late first and early second trimesters. *Ultrasound Obstet Gynecol* **7**: 411-415

172. Vavilala MS, Lee LA, Lam AM (2002) Cerebral blood flow and vascular physiology. *Anesthesiol Clin North America* **20**: 247-64

173. Wehrenberg WB, Chaichareon DP, Dierschke DJ, Rankin JH, Ginther OJ (1977) Vascular dynamics of the reproductive tract in the female rhesus monkey: relative contributions of ovarian and uterine arteries. *Biol Reprod* **17**: 148-153

174. Veille JC, Smith N, Zaccaro D (1999) Ventricular filling patterns of the right and left ventricles in normally grown fetuses: a longitudinal follow-up study from early intrauterine life to age 1 year. *Am J Obstet Gynecol* **180**: 849-858

175. Weiner CP (1995). Intrauterine pressure: amniotic and fetal circulation. In Ludomirski A, Nicolini U, Bhutani UK (eds) Therapeutic and Diagnostic Interventions in Early Life. Chapter IV. Futura Publishing Co Inc. New York, USA.

176. Weiner CP, Heilskov J, Pelzer G, Grant S, Wenstrom K, Williamson RA (1989) Normal values for human umbilical venous and amniotic fluid pressures and their alteration by fetal disease. *Am J Obstet Gynecol* **161**: 714-717

177. Wessels A and Sedmera D (2003) Developmental anatomy of the heart: a tale of mice and man. *Physiol Genomics* **15**: 165-176

178. Wladimiroff JW, Huisman TW, Stewart PA (1991) Fetal and umbilical flow velocity waveforms between 10-16 weeks' gestation: a preliminary study. *Obstet Gynecol* **78**: 812-814

179. Wladimiroff JW, Huisman TW, Stewart PA, Stijnen T (1992) Normal fetal Doppler inferior vena cava, transtricuspid, and umbilical artery flow velocity waveforms between 11 and 16 weeks' gestation. *Am J Obstet Gynecol* **166**: 921-924

180. Wloch A, Rozmus-Warcholinska W, Czuba B, Borowski D, Wloch S, Cnota W, Sodowski K, Szaflik K, Huhta JC (2007) Doppler study of the embryonic heart in normal pregnant women. *J Matern Fetal Neonatal Med* **20**: 533-539

181. Ville Y, Sideris I, Hecher K, Snijders RJ, Nicolaides KH (1994) Umbilical venous pressure in normal, growth-retarded, and anemic fetuses. *Am J Obstet Gynecol* **170**: 487-494

182. Visser GH, Goodman JD, Levine DH, Dawes GS (1982) Diurnal and other cyclic variations in human fetal heart rate near term. *Am J Obstet Gynecol* **142**: 535-544

183. Yao AC, Moinian M, Lind J (1969) Distribution of blood between infant and placenta after birth. *Lancet* **2**: 871-873

184. Yoon H, Shin YS, Lee KC, Park HW (1997) Morphological characteristics of the developing human brain during the embryonic period. *Yonsei Med J* **38**: 26-32

PAPER I

Vimpeli T, Huhtala H, Acharya G. Fetal echocardiography during routine first-trimester screening: A feasibility study in an unselected population. *Prenat Diagn. 2006;26:475-82*.

PAPER II

Vimpeli T, Huhtala H, Wilsgaard T, Acharya G. Fetal cardiac output and its distribution to the placenta at 11-20 weeks of gestation. *Ultrasound Obstet Gynecol. 2009;33:265-271.*

PAPER III

Vimpeli T, Huhtala H, Wilsgaard T, Acharya G. Fetal aortic isthmus blood flow and the fraction of cardiac output distributed to the upper body and brain at 11-20 weeks of gestation. *Ultrasound Obstet Gynecol. 2009;33:538-44.*